TECHNICAL REPORT BRL-TR-3366

BRL

FLOW RESISTANCE IN PACKED AND FLUIDIZED BEDS: AN ASSESSMENT OF CURRENT PRACTICE

C. K. ZOLTANI

JUNE 1992

U.S. ARMY LABORATORY COMMAND

BALLISTIC RESEARCH LABORATORY
ABERDEEN PROVING GROUND, MARYLAND

Destroy this report when no longer needed. Do not return it to the originator.

The findings in this report are not to be construed as an official Department of the Army position unless so designated by other authorized documents.

The contents of this report are not to be used for advertising, publication, or promotional purposes. Citation of trade names does not constitute an official endorsement or approval of the use of such commercial products.

REPORT DOCUMENTATION PAGE

Form Approved
OMB No. 0704-0188

1. AGENCY USE ONLY *(Leave blank)*	2. REPORT DATE	3. REPORT TYPE AND DATES COVERED
	June 1992	Final, Mar 91 - Sep 91

4. TITLE AND SUBTITLE

Flow Resistance in Packed and Fluidized Beds: An Assessment of Current Practice

5. FUNDING NUMBERS

1L161102AH43

6. AUTHOR(S)

C. K. Zoltani

7. PERFORMING ORGANIZATION NAME(S) AND ADDRESS(ES)

8. PERFORMING ORGANIZATION REPORT NUMBER

9. SPONSORING / MONITORING AGENCY NAME(S) AND ADDRESS(ES)

U.S. Army Ballistic Research Laboratory
ATTN: SLCBR-DD-T
Aberdeen Proving Ground, MD 21005-5066

10. SPONSORING / MONITORING AGENCY REPORT NUMBER

BRL-TR-3366

11. SUPPLEMENTARY NOTES

12a. DISTRIBUTION / AVAILABILITY STATEMENT

Approved for public release; distribution is unlimited.

12b. DISTRIBUTION CODE

13. ABSTRACT *(Maximum 200 words)*

Currently used packed and fluidized bed flow resistance models of propellant charges are examined. The underlying assumptions are contrasted and described. Experimental evidence in support for their validity is delineated. Suggestions for the improvement of existing approaches as well as the experimental data still lacking for model development are outlined.

14. SUBJECT TERMS

fluidized bed processes, ignition, ballistics, packed beds

15. NUMBER OF PAGES

67

16. PRICE CODE

17. SECURITY CLASSIFICATION OF REPORT	18. SECURITY CLASSIFICATION OF THIS PAGE	19. SECURITY CLASSIFICATION OF ABSTRACT	20. LIMITATION OF ABSTRACT
UNCLASSIFIED	UNCLASSIFIED	UNCLASSIFIED	SAR

INTENTIONALLY LEFT BLANK.

TABLE OF CONTENTS

LIST OF FIGURES

LIST OF TABLES

INTENTIONALLY LEFT BLANK.

ACKNOWLEDGMENTS

It is a pleasure to thank Messrs. Paul Gough of PGA, Fred Robbins, and Aivars Celmins of the U.S. Army Ballistic Research Laboratory (BRL) for a number of very informative discussions on bed resistance in ballistics. Special thanks go to Doug Kooker, BRL, for comments on an earlier draft of this manuscript and to Malcolm Taylor, BRL, for his insights into nonlinear regression theory.

INTENTIONALLY LEFT BLANK.

1. INTRODUCTION

A considerable number of production methods in the chemical process industry rely on the passage of gases or liquids through beds of particles. Catalytic cracking, drying wet products, producing gas from coal, and pneumatic conveying are typical examples. A huge literature exists describing many facets of this technique (e.g., Howard [1989] and Kunii and Levenspiel [1969]). This knowledge has substantially contributed to our understanding of the early phases of the ballistic cycle when the primer gases convect through the stationary propellant bed and initiate the combustion process. The accuracy of the description of this process depends on a knowledge and the quantification of the losses (i.e., the bed drag). It is our objective here to examine the current approaches to bed drag prediction and scrutinize the assumptions in these theories. We conclude with the presentation of two new models for bed drag which incorporate some of the physics, left out until now, and make recommendations for further research including an outline of experimental data needed.

2. CHARACTERIZATION OF THE BED

The problem to be addressed here is as follows: given a bed of granular particles contained within the walls of a tube open at both ends, determine the pressure loss in a gas which traverses the bed along its axis.

2.1 Description of Bed Constituents. The approach has been to characterize the bed as consisting of closely packed particles. The underlying assumption is that initially the bed is stationary, the particles touch, and no reaction or gas generation is allowed to take place. The particles can assume any shape, but all shapes are normed on that of a sphere. Sphericity, ϕ, also sometimes referred to as Wadell's sphericity factor, is defined as

$$\phi = \frac{\textit{surface area of a sphere of same volume as particle}}{\textit{surface area of particle}}, \qquad (1)$$

For a sphere, the surface to volume ratio is,

$$\alpha = \frac{4\pi(d/2)^2}{4/3\pi(d/2)^3} = \frac{6}{d}, \qquad (2)$$

where d is the particle diameter.

Three different measures of particle diameters are commonly used although at least 12 are known (Allen 1981). For a unimodal distribution of particles, d, the diameter of a particle, suffices. For spherical particles, but polymodal in distribution of sizes, a mean diameter, d_m, is defined. For the distribution of nonspherical particles, a measure incorporating the sphericity is used. Here, the diameter may be defined as d_p = diameter of a sphere having the same volume as the particle, consequently, $d_m = \phi d_p$. Criteria for shape determination, however, are not universal. Due to the irregularity of particle shapes, size is generally determined by sieving. An indication of the variation is sphericity values reported in the literature are shown in Table 1.

Table 1. Variation of Particle Sphericity Values Reported in the Literature

Reference	Particle	Sphericity
Howard (1989)	sand limestone coal	0.92–0.94 0.50–0.90 0.80–0.90
Geldart (1986)	crushed glass	0.65
Kunii and Levenspiel (1969)	sand pulverized coal	0.534–0.628 0.696

In addition, particles are usually categorized according to the Geldart scheme of fluidization behavior (Geldart 1986). For ballistics, two of the categories (B and D) are of interest. Category B, encompassing particles in the size range of 40–500 μm and density range of 1,400–4,500 kgm^{-3}, and category D, for mean particle sizes > 600 μm, are of interest. These require much higher gas velocities for fluidization than the other categories.

It is generally assumed that there is a unimodal distribution of particles in the bed and that the bed is isotropic (i.e., has no preferred direction). Voids are uniformly distributed throughout the bed. The particle size, for spheres given in terms of the radius of the sphere, or for a non-unimodal aggregate expressed as a mean diameter, is given as

$$d_m = \left(\Sigma(x_i/d_i)\right)^{-1} \tag{3}$$

where x_i is the mass fraction of particles of size d_i (i.e., $x_i = n_i(\pi/6)d_i^3/v_p$ where v_p is the volume of the solid particles and n_i is the number of particles of size d_i in the aggregate making up the bed).

The macro view of the bed then is that it can be considered as a collection of small spheroids which constitute the resistance of the passage of a gas stream. The gas enters at one plane of the bed and meanders through the interstices between the particles, then exits at the other end of the contiguous bed. The voidage of the bed, ε, also sometimes referred to as the porosity, is the fraction of the bed which is not occupied by particles. The behavior of the bed depends on the kinds and shapes of the particles present. The losses in the passages manifest themselves as a pressure drop through the bed. The drag of the bed, of course, depends on the path of the gases traversing it. The pathways can be quite elaborate (Carman 1956; Scheidegger 1974). Attempts at modeling the permeability of random media consisting of spheres have been reported recently by Succi, Foti, and Gramignani (1990).

The voids are not distributed evenly throughout the bed, especially near the boundaries, which will be discussed in Section 2.6. Benenati and Brosilow (1962), for example, found that the voidage distribution takes the form of a damped oscillatory wave with the oscillations damped out at about 5 particle diameters from the boundary. For polymodal particle distributions, Jeschar (1964) found that the average void size can be given as

$$\varepsilon = 0.375 + 0.34\, d/D\ , \tag{4}$$

where d is the particle and D the tube diameter.

It is a general rule that the lower the sphericity of the particles in the bed, the higher the voidage. Loose packing gives the greatest voidage while a "tapped" bed results in dense packing. A 10% difference in the voidage values between loose and dense is to be expected. Also, the larger the particle or wider the size spread, the lower the observed voidage in the bed. It is now possible to estimate theoretically the porosity of a bed as a function of the particle size distribution (Yu and Standish 1991). For a randomly packed-bed of spherical particles, the mean voidage is around 0.39. Foumeny and Roshani (1991), based on a series of experiments, found that for equilateral cylinders the mean voidage correlates well with the formula

$$\varepsilon_m = 0.293 + 0.684_r^{-0.85} \left(1 / \sqrt{(1.8837 d_r - 1)} \right) , \qquad (5)$$

where d_r is the tube-to-particle diameter ratio. After a rapid decline at small tube to equivalent volume sphere ratios, there is little variation in the mean voidage when the diameter ratio exceeds 10.

A number of attempts have been reported to give a relationship between velocity and voidage in fluidized beds. The best known, due to Davis and Richardson for liquid-solid sedimentation, has been extended to gas-solid systems by Geldart (1986).

$$U / U^* = \varepsilon^n , \qquad (6)$$

where U^* is the intercept of the log ε – log U plot at $\varepsilon = 1$. Values for n have been reported ranging from 3.84 to 19.7. Generally, n increases with decreasing particle size below 60 μm. Hirata and Bulos (1990), for solid-liquid fluidization based on 811 data points, suggested a new correlation,

$$\varepsilon = \varepsilon_{pk} + (1 - \varepsilon_{pk}) \varepsilon_{rz}^A \exp(B(1 - \varepsilon_{rz})) , \qquad (7)$$

with $A = 2.2n + 8d_p/D$, $B = 2.1n$ and which shows a deviation of less than 5%. Here ε_{pk} is the packed-bed and ε_{rz} the bed voidage based on the Richardson-Zaki type equation, n the

Richardson-Zaki exponent. An alternative approach, based on the Carmen-Kozeny equation, exists; but rather large scatter in the data have been reported.

2.2 Bed Flow Model. The gases from the igniter penetrate the packed-bed and, seeking the route of least resistance, reach the base of the projectile. During this process, the propellant ignites and creates additional mass sources for the gas, resulting in an appreciable pressure rise. When the frictional resistance of the projectile is overcome, the projectile moves, leading to a fluidized particle-gas mixture down the tube.

Bed drag resistance when the bed is still stationary, can be characterized by several parameters, the most important of which are the friction factor, void friction, and, of course, the Reynolds number of the gas flow.

In the absence of gas generation within the aggregate, the pressure drop through the bed increases linearly with the gas velocity until fluidization takes place. Thereafter, the pressure in the bed remains fairly constant until such time the flow velocity approaches the terminal velocity at which point the pressure drop across the bed vanishes.

2.2.1 Darcy's Model. The simplest model of bed resistance is based on Darcy's model of flow through an aggregate. It relates the volumetric flow rate to the energy losses—inversely to the length of the bed, and proportionately to a permeability coefficient. The relationship is empirical; it was not derived from first principles though ex post facto, a number of attempts have been made to justify it on basis of the Navier-Stokes equation. Originally intended for $Re_p < 1$, where Re_p is the Reynolds number based on the particle diameter, in differential form it is

$$Q/A = -k/\mu(dp/dx) \tag{8}$$

where Q is the volume flow rate, μ is the viscosity of the fluid, and k represents the permeability. This is a lumped parameter model and hides much of the physics of the flow process.

Strictly, Darcy's model is applicable only in the very low velocity domain. When the linear relationship between the pressure gradient and the velocity no longer holds, more general relationships must be used. Claims of validity range from 0.1 up to almost 100 in the Reynolds number. The large variance can be explained partially based on the fact that the length scale adopted is not the same in all the models.

Considerable literature exists on the Darcy equation and attempts at extending its region of applicability. An insight into some of the issues surrounding it is given in Mannsett (1991). The search for a solution of the equation is aided by the fact that it is of the heat transfer type (i.e., parabolic in nature). Many techniques exist for its solution. The unsteady and more interesting form of the equation is, however, more challenging.

There are three unknowns—velocity, density, and pressure. To determine the flow pattern within a porous bed, Equation 8 must be supplemented by an equation of state, i.e., a relation between pressure and density and a continuity equation where U is the superficial velocity, i.e.,

$$\varepsilon \partial \rho / \partial t = div U \rho \ . \tag{9}$$

The equation which then can be solved for p follows:

$$\varepsilon \partial \rho / \partial t = div[(\rho k/\mu)(gradp - \rho g)] \ , \tag{10}$$

where the coordinate system was chosen with g pointing downward.

For steady-state flows, the left side of Equation 10 is set equal to zero. If homogeneity and incompressibility can be assumed, considerable simplification ensues. This approach has been explored in detail by oil companies to calculate, for example, flow from oil bearing strata into a well.

In the unsteady case, through appropriate linearization, the equation can be brought into the form of the heat conductivity equation. Thus, a whole array of methods becomes available for the solution of transient flow in a porous bed.

Due to the difficulty of describing the flow in the interstices among the propellant grains, historically a more heuristic and less mathematical approach was taken. These, starting with some definitions, are described in the following sections.

2.2.2 Friction Factor. The friction factor in a channel is defined as the pressure drop per diameter divided by the dynamic pressure at entry,

$$f = \tau_w / (1/8)\rho U^2 \ . \tag{11}$$

Here, τ_w is the wall stress. Bird, Stewart, and Lightfoot (1966) extended the idea to packed-beds by using the particle diameter as the length scale, so that

$$f = \frac{grad\, p}{0.5\rho u^2} \frac{d_p}{4L} \ , \tag{12}$$

where d, the particle diameter, is also the length scale; U the velocity, also sometimes referred to as the superficial velocity (i.e., the velocity without particles present); and L the length of the bed. Darcy's law then can be brought to the following form valid for $Re < 4$,

$$f = C/Re \ . \tag{13}$$

For $4 < Re < 180$, the following relationships have found acceptance

$$fRe = aRe + b \ , \tag{14}$$

where the constants a and b assume the values 40 and 2,500. For $10 < Re < 300$, the following formula holds

$$f = 94/(Re)^{0.16} \ . \tag{15}$$

It appears that Chalmers, Taliaferro, and Rawlins (1932) were the first to introduce the concept of porosity into the friction factor. That is,

$$f = gradpd\,\varepsilon^2/(\rho U^2) \ , \tag{16}$$

where ε is the porosity. Shortly thereafter, Barth and Esser (1933) proposed a relationship valid for $5 < Re < 5{,}000$,

$$f = 490/Re + 100/(Re)^{0.5} + 5.85 \ . \tag{17}$$

Ergun's model, to be discussed further, incorporated a voidage factor, i.e.,

$$f = \frac{K_1(1-\varepsilon)}{Re} + K_2 , \tag{18}$$

where K_1 usually is taken as 150 and K_2 as 1.75. Other relevant references are El-Kaissy and Homsy (1973) whose relationship is valid for $0.3 < \varepsilon < 0.6$ and Nishimura and Ishii (1980) who surprisingly found that for $0.3 < \varepsilon < 1.0$, the pressure drag coefficient is independent of *Re*. (See also Jaiswal, Sundararajan, and Chhabra [1991]).

To put these relationships and values of *f* in context, it is useful to recall that, in pipes or plates, *f* numbers tend to be in the thousands when *Re* is very small, $1 < f < 3$ for $Re = 1{,}000$ and 0(1) at higher *Re*. The Blasius formula, valid for $10^3 < Re < 10^5$, *f* varies with $(Re)^{-0.25}$. In laminar flow, $f = 16/Re$ and, interestingly, C_D, is a multiple of *f* at low *Re*.

Rowe (1961) makes the interesting observation that for water flowing through an array of spheres, the force on a single sphere in the array was 68.5 times the force on an isolated sphere for the same value of the superficial velocity. Surprisingly, this relationship appears to be true at elevated Reynolds numbers and is useful in determining the void fraction at fluidization as it is discussed later.

2.3 Single Particle Drag and Its Extension. At higher Reynolds numbers, an approximation of the bed drag can be obtained by starting with a single particle, obtaining the drag relationship, and then generalizing to a bed. The drag on a particle in a medium of infinite extent can be written as

$$F = C_D(\rho U^2/2)(\pi d^2/4) \ . \tag{19}$$

Here C_D is the drag coefficient and ρ the density of fluid. The number of particles present in a bed can be expressed as

$$N = AL(1-\varepsilon)/(\pi d^3/6) \ , \tag{20}$$

where A is the area and L the length of the bed so that the drag force of N particles becomes

$$F = \Delta PA/(Nf(\varepsilon)) \ , \tag{21}$$

where $f(\varepsilon)$ is the voidage function, usually determined experimentally. For values of ε in the range $0.3 < \varepsilon < 0.7$, the following relationship (Watanabe 1989) has been suggested:

$$f(\varepsilon) = 25(1-\varepsilon)/3\varepsilon^3 \ . \tag{22}$$

Combining Equations 19–21, the following relationship is obtained:

$$C_D Re^2 = [(4/3)/((1-\varepsilon)f(\varepsilon))][d^2\rho][\Delta p/L] \ . \tag{23}$$

The drag coefficient for simple spherical shapes can, in general, be expressed in the form

$$C_D Re^a = b \ , \tag{24}$$

where a and b are constants at a particular Reynolds number. Substituting back into Equation 23, we get

$$Re = f(\Delta p/L)^n \ , \tag{25}$$

where n = constant.

In the laminar regime, $C_D Re = 24$ and, assuming the voidage function cited above, one obtains the Carman-Kozeny relationship.

$$\Delta p/L = K\mu/d_{sv}^2[(1-\varepsilon)^2/\varepsilon^3]U \ , \tag{26}$$

where U is the superficial velocity, $K = 180$, $0.4 < \varepsilon < 0.5$, and $0.1 < Re < 1$. d_{sv} is the diameter of a sphere having the same extended surface/volume ratio as the particle.

For turbulent flow with $C_D = 0.44$, Equation 26 transforms into the Burke-Plummer equation. Adding the Carman-Kozeny and Burke-Plummer equations, Ergun's equation is obtained. Rearranging the latter,

$$\Delta p/L = (\mu U/d^2)((1-\varepsilon)^2/\varepsilon^3)] + 1.75(\rho U^2/d)(1-\varepsilon)/\varepsilon^3 \ . \tag{27}$$

Comparing Equation 27 with Equation 23, an equivalent bed drag coefficient can be obtained. Thus, the drag coefficient of the bed when $\varepsilon = 0.44$ in the laminar region is

$$f = 24/Re + 0.5 \ . \tag{28}$$

Several other forms, depending on the C_D form assumed (i.e., the Re regime), have been derived. (See for example Watanabe [1989]).

Each of these models assume some knowledge of the geometry of the granules making up the bed and the function describing the drag coefficient. Table 2 illustrates the wide variation in C_D with Re which have been proposed for single spheres. (See also Davidson, Clift, and Harrison [1985]). Data on nonspherical objects are scarce at best.

When the particles are in close proximity, as in a bed, the single particle, unbounded flow drag correlations are modified. Indeed, the effects of void fraction ε has been included in

Table 2. Variation of C_D With Re - Single Particle Spheres

Reference	Correlation	Remarks
Clift, Grace, and Weber (1978)	$C_D = 3/16 + 24/Re$	$Re < 0.01$
	$C_D = 24/Re[1 + 0.131Re^{0.82 - 0.05w}]$	$0.01 < Re < 20$
	$C_D = 24/Re[1 + 0.1935Re^{0.63}]$	$20 < Re < 260$
	$C_D = 0.19 - 8 \times 10^4/Re$	$10^6 < Re$ where $w = log_{10}Re$

some coefficient correlations, as discussed in Section 2.2.2 (Poo and Ashgriz 1991). Typically, for a bed,

$$C_D = 24/Re(\varepsilon^{-2.65} + [Re^{0.66}\varepsilon^{-1.78}/6]) , \tag{29}$$

which also shows that the drag coefficient increases when the volume fraction, here for liquid droplets in a gas stream, increases. Overall, at lower Re numbers, a reduction in drag coefficient for aligned spheres and an increase for adjacent spheres have been reported (i.e., the closer the spacing, the lower the coefficient). The drag coefficient is very sensitive to both the lateral and vertical spacing of the particles, *a functional relationship* expressing the dependence of C_D on Re, spacing, and drop size has been proposed. Wen and Yu (1966) found that, based on fluidized bed measurements,

$$C_D = \varepsilon^{-2.7}[24/(\varepsilon Re) + 3.6/(\varepsilon Re)^{0.317}] , \tag{30}$$

and Pike (1990), for intermediate porosity regimes and $Re > 10^2$, suggested the expression

$$C_D = \varepsilon^{-2.7}[C_{DS}(\varepsilon Re) + \varepsilon Re(1 - \varepsilon)(5\varepsilon - 2.2)/100 + \varepsilon Re] . \tag{31}$$

This expression is valid for $0 < Re < 10^5$. As of this writing, this is an active area of research. These issues also have great importance for spray flow analysis.

2.4 The Bed as an Aggregate of Flow Channels. There are several possible approaches to modeling the pressure drop through a stationary porous bed. In one case, the particles are

looked upon as submerged objects with flow taking place around them and, in the other, due to Kozeny and the usually preferred way, the porous bed is represented as an assemblage of pipes of various lengths and cross-sectional areas. The pipes can be twisted, the cross sections are not necessarily circular, and their length can be greater than the bed depth. The underlying hypothesis is that the important parameter in the problem is the surface area of the particles (i.e., the surface area with which the gas comes in contact in its passage through the bed). It has been variously estimated that 1 m^3 of 100-μm particles have a surface area in the neighborhood of 30,000 m^3. The total surface area of the particles is set equal to the inside surface area of the tubes conducting the gas which is passing through the bed. The losses are assumed to be similar.

Not all conduits are cylindrical in shape; therefore, an equivalent radius, the hydraulic radius

$$R_h = A/P \ , \tag{32}$$

where A is the cross-sectional area open to the flow and P the perimeter of the wetted surface, was introduced.

The use of the mean hydraulic radius is predicated to hold on the following conditions:

(1) the wall of the tube is straight and only wall shear stress acts;

(2) the shear stress is constant at each point on the wall; and

(3) equilibrium conditions prevail (i.e., the shear stress times the tube surface area is equal to the pressure drop times the tube cross-sectional area).

The drag on the walls of a pipe, as a consequence of flow in it, on the other hand, is derived simply by equating the pressure drop across a cylinder of fluid to the viscous stresses, τ_w, acting on the walls. Simple algebra shows that

$$\tau_w = (p - p_o) D/(4L) \ . \tag{33}$$

The pressure drop through the bed, modeled on the basis of a series of parallel tubes, can be approached in two ways. In the first, starting with the relationship expressing drop in a tube and assuming laminar flow, and the hydraulic radius given in terms of the void fraction, i.e.,

$$R_h = \frac{\textit{volume of voids / volume of bed}}{\textit{wetted surface / volume of bed}} . \tag{34}$$

Now, let U be the superficial velocity, also sometimes referred to as the Dupuit velocity (i.e., the velocity which would be present in the absence of particles in the conduit), and v the velocity in the interstices of the bed

$$v = U/\varepsilon . \tag{35}$$

From the Hagen-Poiseuille formula, the superficial velocity in the bed is

$$U = \Delta p/(2\mu L) R_h^2 \varepsilon , \tag{36}$$

$$U = (\Delta p/L)(d_p^2/[(72\mu)])(\varepsilon^3/(1-\varepsilon)^2) . \tag{37}$$

This equation is valid for $\varepsilon < 0.5$. It has been found that agreement with observations is improved when the factor 72 in the right-hand side is more than doubled. Thus, finally

$$U = \Delta p/L(d_p^2/150\mu)[\varepsilon^3/(1-\varepsilon)^2] , \tag{38}$$

which is also known as the Blake-Kozeny formula and corresponds to a bed friction factor of

$$f = [(1-\varepsilon)^2/\varepsilon^3]75/[(d_p G_o)/\mu] , \tag{39}$$

where we have set $G_o = \rho U$ and used the definition of the friction factor and the Hagen-Poiseuille formula.

In the turbulent regime, an analogous approach leads to the Burke-Plummer equation (Bird, Stewart, and Lightfoot 1966),

$$\frac{\Delta p}{L} = 3.5 \frac{\rho U^2}{2 d_p} (1 - \varepsilon)/\varepsilon^3 , \tag{40}$$

and corresponds to a friction factor of

$$f = 0.875(1 - \varepsilon)/\varepsilon^3 . \tag{41}$$

$(1 - \varepsilon)/\varepsilon^3$ is the Kozeny porosity function. When Equations 38 and 40 are added together, the Ergun equation is obtained. It should be noted that for high flow rates the first term on the right becomes negligible and the Burke-Plummer equation holds.

The main criticism of the Kozeny model is that it does not account for the influence of the expansions and constrictions of the channel on the flow.

2.5 Ergun's Approach. In an alternative approach, first suggested by Forchheimer (1901) for water seeping through soil and later expanded by Ergun (1952), it is assumed that along the flow direction through the bed

$$dp/dx = \alpha v + \beta v^2 , \tag{42}$$

where α and β are dimensionless factors determined from experiments. dp/dx is the pressure drop over a length L in a single tube of diameter d, set equal to the particle diameter, obtained on the basis of Hagen-Poiseuille (i.e., laminar flow).

$$\Delta p/L = 32 \mu v/d^2 , \tag{43}$$

where v is the mean fluid velocity.

The pressure drop due to dissipation of kinetic energy in the turbulent eddies is taken as

$$\Delta p/L = 1/2\rho v^2/d \ . \tag{44}$$

The total pressure drop in the bed becomes

$$\Delta p/L = 32\mu v/d^2 + 1/2d\rho v^2 \ . \tag{45}$$

Now, using the definition for the superficial (i.e., empty tube) fluidizing velocity

$$v = U/\varepsilon \ , \tag{46}$$

and the fact that

$$d = \frac{4\varepsilon}{1-\varepsilon}\left(\frac{1}{S_v}\right), \tag{47}$$

(assuming that the surface area of particles to the void volume is the same as the tube surface area of N tubes to the volume of fluid flowing through the cluster of tubes), the tube diameter can be expressed in terms of void volume and S_v, the surface area per unit volume

$$\frac{\Delta p}{L} = \frac{\alpha\mu S_v^2 U}{\varepsilon}\frac{(1-\varepsilon)^2}{(16\varepsilon^2)}32 + \frac{(1-\varepsilon)}{\varepsilon^3}\frac{S_v U^2}{8}\rho\beta \ , \tag{48}$$

$$d_m = 6/S_v \ ;^* \tag{49}$$

therefore,

$$\frac{\Delta p}{L} = 72\alpha\frac{(1-\varepsilon)^2}{\varepsilon^3}\frac{\mu U}{d_m^2} + \frac{3\beta}{4}\frac{(1-\varepsilon)}{\varepsilon^3}\frac{\rho U^2}{d_m} \ . \tag{50}$$

---

* Recall that S_v = surface/volume = $6/d_m$.

Again, from experimental data using a value for α such that $72\alpha = 150$ and a value of β such that $1.75 = 3\beta/4$, the Ergun equation is obtained. For nonspherical particles, d_m is replaced by ϕd so that

$$\frac{\Delta p}{L} = 150 \frac{\mu U}{\phi^2 d^2} \frac{(1-\varepsilon)^2}{\varepsilon^3} + \frac{1.75}{(\phi d)} \rho U^2 \frac{1-\varepsilon}{\varepsilon^3} . \tag{51}$$

Thus, knowing U, ε, d_m, ϕ, and L, the pressure drop (Δp) throughout the bed can be predicted. But, it should be noted that there are a number of ad hoc assumptions in the derivation of Equation 51 which limits the applicability. It is unlikely that these assumptions are met in many flows of ballistic interest.

In differential form in terms of the mass velocity, $G = \rho U$, the pressure drag can be written as

$$\frac{dp}{dz} = -(aG + bG^2) \tag{52}$$

where z is the axial coordinate and

$$a = 150 \frac{(1-\varepsilon)^2}{\varepsilon^3} \frac{\mu}{d_p^2 \rho} \tag{53}$$

$$b = 1.75 \frac{(1-\varepsilon)}{\varepsilon^3} \frac{1}{d_p \rho} . \tag{54}$$

The minus sign, as usual, indicates that the pressure is dropping in the direction of increasing z. Some authors (Rase 1990) advocate that, for rough beads in the bed, the factor 150 should be replaced by 180 and 1.75 by 4.0.

The Ergun equation loses its validity as the Reynolds number increases, long before the onset of fluidization. For the whole bed in motion, a modified Ergun relationship has been

proposed by Yoon and Kunii (1970). A test of this formulation for the bed resistance just after the projectile commences its motion and before the bed is fluidized still needs to be performed. Also, note that there are a number of ad hoc assumptions in the derivation of Equation 51 which limits its applicability to a real ballistic flow.

2.6 Effect of the Wall on the Correlation. The effect of bounding walls on the drag of a single particle has been discussed by Clift, Grace, and Weber (1978). Defining

$$K_F = \frac{\textit{drag in bounded fluid}}{\textit{drag in infinite fluid}} = \frac{F_D}{F_{D\infty}} , \tag{55}$$

the fractional increase in drag caused by the wall effects then is given by $K_F - 1$. For Reynolds numbers of up to 50, C_D is given by the following relationship suggested by Fayon and Happel (1960):

$$C_D = C_{D\infty} + (24/Re)(K-1) , \tag{56}$$

where K is the wall correction factor and $C_{D\infty}$ is the drag coefficient in an infinite fluid. Its value is given as

$$K = [(1 - 0.475\lambda)/(1 - \lambda)]^4 , \tag{57}$$

where λ is the particle to the tube diameter ratio. In the regime $10^2 < Re < 10^4$, K_F has been found to be independent of Re and is given within 6% by

$$K_F = 1/(1 - 1.6\lambda^{1.6}) \text{ for } (\lambda < 0.6) . \tag{58}$$

At $Re > 10^5$, Achenbach (1974) recommends

$$K_F = (1 + 1.45\lambda^{4.5})/(1 - \lambda^2)^2 , (\lambda < 0.92) . \tag{59}$$

In addition to the effect of the walls on the drag on the particle, the particle alters the shear on the duct. At low particle Reynolds numbers and for particles small in comparison with distance between particle and the wall, an excess pressure drop can be observed. Clift, Grace, and Weber (1978) and Happel (1958) give more details.

The effect of bounding walls on bed drag has been explored in some detail in Fond and Thinakaran (1990), Mehta and Hawley (1969), Reichelt (1972), Roblee, Baird, and Tierney (1958), Schwartz and Smith (1953), and Tosun and Mousa (1986). Considerable evidence points to the fact that the presence of the wall changes the porosity nearby by forcing the particles to arrange themselves to conform to the shape of the wall. In the case of spherical particles, porosity tends to 1 as the wall is approached. In a zone of 3–5 particle diameters from the wall, the porosity varies cyclically and, therefore, assumes greater values than near the center of the tube. Confirmation of this observation has also been furnished by Dr. Foumeny of Leeds University (Hewitt 1991) who, using image and computer graphics analysis, verified the cyclic variation of the void fraction near the wall and, thus, the presence of the wall-channeling effect.

The significance of this observation is that, for smaller D/d_p ratios, the annular region of higher porosity takes a larger percentage of the cross-section area available for flow. Indeed, the gas velocity through a packed bed assumes a maximum value, which can be twice the centerline velocity at about 1 particle diameter from the pipe wall (Schwartz and Smith 1953).

Only for $D/d_p > 40$ does the effect of the wall lose its importance (Fond and Thinakaran 1990). For ballistic packed beds this is significant, since in many cases with particle size of the order of a centimeter and tube widths of 10–15 cm, wall effects are definitely present.

Mehta and Hawley (1969) and Reichelt (1972) proposed modified versions of the Ergun equation to take account of the wall effect. Defining a hydraulic radius R_h as

$$R_h = \frac{\varepsilon d}{6(1-\varepsilon)M}, \tag{60}$$

where

$$M = 1 + 2/3[d/(D\{1-\varepsilon\})] , \tag{61}$$

the relationship

$$f_w Re_w = A_w + B_w Re_w , \tag{62}$$

was obtained. For $0.2 < Re_w < 30{,}000$, $A_w = 150$ and B_w was defined for

$$1/\sqrt{B_w} = 1.5/[D/d]^2 + 0.88 . \tag{63}$$

As usual, f is the friction factor and Re the modified Reynolds number (i.e., Re divided by $(1 - \varepsilon)$). Here the subscript w is used to emphasize the reference to the wall. Finally, Rase (1990) suggested multipliers for small tubes, though smallness is not defined. For a uniform normal charge of spheres with $\varepsilon = 0.4$, the void fraction multiplier is $1 + 0.42\, d_p/D$.

2.7 Effect of Mass Transfer on the Drag in the Boundary Layer. Once the ignition stimulus in the form of gases spreading through the propellant bed appears, mass evolution from the propellant surface commences. Flow along a surface in the presence of mass transfer can, and usually does, differ markedly from inert flow. Values of heat transfer and drag coefficient are affected. Specifically, mass transfer away from a body tends to reduce the viscous drag but also increases the pressure drag.

Important references are Spalding (1954), Emmons (1956), Eisenklam, Arunachalan, and Weston (1967), Yuen and Chen (1978), Renksizbulut and Haywood (1988), and Raju and Sirignano (1990). The basic mechanism at work is well illustrated by the evaporation of droplets in a convective environment. In the following, we confine our observations mainly to this case since it captures most, if not all, important facets of the problem. Two processes are of importance here: evaporation which changes the composition of the gas phase and leads to significant changes in the thermophysical properties and, thus altered heat, mass, and momentum transfer rates. Also, evaporation produces nonuniform blowing at the surface resulting in a lowering of the heat transfer to the propellant and a reduction in friction drag but an increase in the pressure drag. We recall that the total drag, C_D, is made up of the friction

drag, C_f, the pressure drag, C_p, and a thrust drag, C_t, calculated at the surface. C_t is caused by the nonsymmetrical surface mass flux. Usually it makes up less than 5% of the total drag. Generally, the pressure drag predominates. Friction drag, C_f, in the presence of mass transfer, decreases due to the fact that surface blowing dramatically reduces velocity gradients at the surface. Heat transfer into the solid and the presence of a liquid film, if there is one, further complicates the analysis.

Consider a particle in a gas stream whose temperature is high enough to induce evaporation from the particle. Several factors are expected to alter the transfer coefficients at the surface of the drop. Evaporation reduces the film drag due to a thickening of the boundary layer and, if combustion is also present, form drag is modified by the combustion products. Of course, the temperature and concentration gradients will also impact upon the location of the boundary layer separation point and, thus, the value of the drag. Large reductions in drag coefficients have been reported in the literature; thus, this effect cannot be ignored.

The effect of evaporation on friction drag on a flat plate has been studied by Emmons (1956) who was able to show that, for a mass transfer number B below 4, the quantity $C_f Re^{0.5}(1 + B)^{0.75} = 1.328$ to within 5%. Thus, evaporation reduces the friction drag, C_f, by the factor $(1 + B)^{0.75}$. Similar results have been obtained for flow past spheres at low Reynolds numbers.

Due to the transient and multicomponent nature of droplet evaporation, quantitative predictions have been attempted only under idealized conditions. The analysis is made difficult by the fact that flow transitions around the particle are thought to occur, necessitating recourse to numerical solutions. Renksizbulut and Haywood (1988) indicate that

$$C_D(1 + B)^{0.2} = (24/Re)\,(1 + 0.2\,Re^{0.63}) \ , \qquad (64)$$

valid the regime $10 < Re < 300$. Re is based on the relative velocity. B, the transfer number (sometimes referred to as the Spalding number), is defined as

$$B = (T_\infty - T_s)/L^* c_p \,, \tag{65}$$

where s refers to the surface, ∞ to the free stream conditions, and L^* is the latent heat of vaporization of the droplet. Alternatively, B is sometimes defined in terms of mass fractions. B then represents the ratio of the driving force to the resistance of interphase transfer. From the heat transfer standpoint, the driving force is constituted by the heat released per unit mass of oxidizer and the difference in enthalpy per unit mass between the ambient and gas at the surface. The resistance consists of the heat of evaporation per unit mass of fuel vaporized. When a surface (or droplet) vaporizes, gas phase diffusion of the fuel (instead of heat conduction) can be the driving force; thus, B can be expressed in terms of mass fraction. The viscosity is determined according to the one-third rule (i.e., superior correlations are obtained when the reference temperature is evaluated closer to the wall than the film value).

The left side of Equation 63 accounts for the reduction in drag due to blowing and evaporation, while on the right side, the standard form for flow over spheres at the indicated Re is given. Thus, once the reaction (i.e., the gas evolution with the bed commences), the use of inert C_D values can introduce substantial errors into the bed drag calculations. A number of correlations of mass transfer in packed beds exist (Rase 1990; Geankoplis 1983).

The caveat emptor here is that this theory and the supporting experiments were done at Re numbers considerably lower than those which are of interest for propellant bed drag studies. However, even here, blowing takes place and it will have an effect on the level of drag as the gas makes its way through the aggregate.

2.8 Criteria for Fluidization. Early on, researchers have observed that for low gas approach velocities, a linear relationship exists between the pressure drop through the bed and the velocity. When the flow becomes turbulent, the velocity dependence becomes nonlinear. At the fluidization velocity, the particles are no longer in contact with each other and the pressure drop across the bed times the bed cross-sectional area is exactly counterbalanced by the weight of the bed. An increase in pressure rise is no longer observed but, on the whole, stays constant until the velocity is increased to the point that the particles actually become airborne—at which point the bed pressure drops back to zero. This is

observed at the so-called "terminal velocity" of a typical particle. The terminal velocity, also called the "free fall" velocity of a particle U_t, is determined by performing a force balance on an individual particle and then calculating the velocity that it would eventually reach. Typically, in an unbounded flow, the force balance on a spherical particle reads as

gravitational force – drag force – buoyancy = accelerating force.

The drag force is given by

$$F = C_D A 1/2 \rho U^2 , \tag{66}$$

where C_D is the drag coefficient and A is the area of the sphere facing the flow. The force relationship on the particle can be expressed as

$$(\pi/6)(\rho_p - \rho_f) d_p^3 g - F = \pi d_p^3 \rho_p dU/dt . \tag{67}$$

At the terminal velocity (the accelerating force is zero), Equation 67 reduces to

$$F = (\pi/6) d_p^3 (\rho_p - \rho_f) g . \tag{68}$$

Combining and solving,

$$C_D = (4/3)(\rho_p - \rho_f) d_p g/(\rho_f U_t^2) . \tag{69}$$

In the laminar region, Stokes' law,

$$F = 3\pi\mu U d_p , \tag{70}$$

holds and, when substituted back into Equation 67, yields the familiar expression for the terminal velocity

$$U_t = (\rho_p - \rho_f) g d_p^2 / (18\mu) \ . \tag{71}$$

In the turbulent regime, for particles larger than 1,500 μm, $C_D = 0.43$ and

$$U_t = \sqrt{(4/3)(\rho_p - \rho_f) g d_p / (0.43\rho_f)} \ . \tag{72}$$

It should be noted that viscosity does not enter into the equation.

For nonspherical particles, a correction factor has been introduced. It should be recalled that equal values of sphericity do not necessarily imply the same shape and, thus, their aerodynamic behavior will also differ. In the turbulent regime, a correction factor for sphericities in the range from 0.67 to 0.906,

$$K_{ns} = 5.31 - 4.88\phi \ , \tag{73}$$

is included in the denominator of Equation 70.

A representative sampling of gas-solid correlations at minimum fluidization velocity from the literature is given in Table 3. Here U_{mf} is the minimum superficial velocity at fluidization, ϕ the shape factor, *Mv* the density ratio, $(\rho_p - \rho_f)/\rho_f$. It should be kept in mind that these formulae are not expected to apply exactly to a ballistic event. While in many industrial processes the columns are open at both ends and flow is against the pull of gravity, in a gun, flow down the tube only commences when the gas pressure overcomes the inertia of the projectile whose axis is in a plane a few degrees from the horizontal. A criterion for fluidization for the propellant bed is not known to the present writer.

A characteristic of gas-fluidized beds is that they tend to be nonhomogeneous and void volumes are created (Davidson, Clift, and Harrison 1985). At small void size values, agitation of the bed is observed. This is quite different from liquid-particulate systems.

Table 3. Gas-Solid Correlations at Minimum Fluidization Velocity

Reference	Correlation	Remarks
Leva (1959)	$U_{mf} = 7.21x10^{-4} d^{1.82} (\rho - \rho_f)^{0.94} g / (\rho_f^{0.06} \mu^{0.88})$	sand
Kunii and Levenspiel (1969)	$Re_{mf} = k_o^2 \varepsilon_{mf}^2 GaMv / (150(1 - e_{mf}))$	$Re_{mf} < 20$
Davidson, Clift, and Harrison (1985)	$Re_{mf} = 11.95x10^{-2} (GaMv)^{0.66}$	$30 < Re_{mf} < 180$

Criteria for fluidization in a propellant bed is only implicitly defined in the literature. Gough (1977) gives values for the interphase drag in terms of the void fraction and ε_o, where ε_o is the settling porosity and

$$\varepsilon_1 = [1 + 0.02(1 - \varepsilon_o)/\varepsilon_o]^{-1} . \tag{74}$$

$$f = 1.75 , \qquad \varepsilon < \varepsilon_o \tag{75a}$$

$$f = 1.75 [(1 - \varepsilon)/(1 - \varepsilon_o)(\varepsilon_o/\varepsilon)]^{0.45} , \qquad \varepsilon_o < \varepsilon < \varepsilon_1 \tag{75b}$$

$$f = 0.3 , \qquad \varepsilon_1 < \varepsilon \leq 1 \tag{75c}$$

When $\varepsilon > \varepsilon_1$, Gough postulates that the appropriate friction factor is that of an isolated sphere and thus (75c) becomes operative.

2.9 Effect of Bags on the Bed Resistance. The case of bagged charges is complicated by the added resistance of the bag to the gas flow. Of course, the bag burns up quickly, therefore, its effect is transitory. A possible quantification of this effect is the approach of Spielman and Goren (1968) who showed that the resistance of a canvas bag to the passage of gases can be expressed by the following implicit relationship:

$$ka^2 = 4\alpha f(Kn, ka^2) , \tag{76}$$

where Kn is the Knudsen number, a the fiber radius, α the volume fraction of the fiber, and k the Darcy coefficient. The theory is based on the assumption that, near the fibers, Stokes equation applies but, at greater distances, Darcy's equation takes over.

2.10 Void Center Cores and Spouted Beds. An analogy between the flow through a spouted bed and a propellant with void center core can be established. Spouted beds consist of coarse particles—usually 500 μm or larger. The gas enters the bed by means of an entry nozzle or orifice plate and forms a cylindrical cavity which penetrates through the bed. The passage way of the gas is usually referred to as the "spout." The gas, of course, also spreads radially into the annular bed region. The particles are lofted and eventually fall back into a downward, annulus bed of solids.

Spouted beds are preferred for many applications since the pressure drop through the bed is lower than in a regular fluidized bed and, for coarse particles, contact between the phases is better than in a fluidized bed. Spouted beds are discussed at length in Epstein and Levine (1978) who modified the Mamuro-Hattori theory by dropping the proportionality between the pressure gradient and the velocity, as is assumed in Darcy's law. That is, instead of

$$-dp/dx = kU \,, \tag{77}$$

the more general relationship,

$$-dp/dx = k_1 U + k_2 U^2 \,, \tag{78}$$

where k_1 and k_2 are the coefficients in Ergun's equation, is adopted. Substituting this equation into a relationship giving the force balance of a differential slice of the annulus, a differential equation is obtained which, with the appropriate boundary conditions, can be solved in a straight forward manner for the pressure drop through the bed.

2.11 The Standpipe Analogy. Once the projectile starts to move, the fluidized propellant bed may be looked upon as having some similarities to a standpipe flow. Standpipes are utilized in hydrocarbon cracking plants, the Fischer-Tropsch process, and in coal gasification.

Considerable literature exists on the subject. Standpipes may be oriented vertically or at some angle and facilitate the downflow of particulate solids.

There are two regions of interest: the fluidized, where

$$U_{sl} > U_{mf}/\varepsilon_{mf} \, , \; \varepsilon > \varepsilon_{mf} \, , \tag{79}$$

and the nonfluidized with

$$U_{sl} < U_{mf}/\varepsilon_{mf} \, , \; \varepsilon < \varepsilon_{mf} \, . \tag{80}$$

(Subscript *mf* denotes minimum fluidization.)

The mathematical modeling of standpipe flow also proceeds from the modification of the Ergun equation (Yoon and Kunii 1970) and the use of a solid mixture momentum equation,

$$dp/dx = k_1 U_{sl} + k_2 U_{sl} \mid U_{sl} \mid \, , \tag{81}$$

where k_1 and k_2 are the usual constants in the Ergun equation and U_{sl} is the slip velocity defined as

$$U_{sl} = U_g/\varepsilon + U_s/(1-\varepsilon) \, , \tag{82}$$

where U_g is the superficial gas velocity and U_s is the superficial solid velocity. A large number of correlations of U_{sl} exist (Leung and Jones 1978).

For moving a solid mixture, Hinze (1968) obtained a relationship relating the stress in the solid to the stress on the confining tube wall.

2.12 Transition of Turbulence. Fundamental changes in the bed structure are observed when the velocity becomes high enough for the flow to be turbulent. The velocity at which this is thought to occur is defined as the "transition velocity." The significant observation at

this juncture in the evolution of the flow is demixing of gas and solid particles. For small particles, the transition velocity is fairly low, but for coarse, larger particles, this velocity tends to be high. Here, the resulting flow is marked by wide channels and demixing patterns.

The demixing regime is characterized by a leveling off of the pressure fluctuations and loss of periodicity in the capacitance probe values when the flow is monitored. The transition velocity generally decreases with pressure and with an increase in the bed size. In the conventionally fluidized bed at transition, a breakdown of the slugs into smaller bubbles is observed as well as a homogenization of the flow. The ratio of the transition to the terminal velocity decreases with particle size and density but is generally > 1 for the fine particles and in the range of 0.3–0.35 for coarse, large particles (diameter ≥ 2,600 μm).

The propellant bed at the verge of transition from laminar to turbulent flow has not been investigated, either theoretically or experimentally, in any detail. Some trends of the expected behavior can be gleaned from the literature on high-velocity fluidized beds (Geldart 1986).

2.13 Scaling. Considerable progress in the understanding of fluidized bed behavior has been achieved based on small-scale experiments. Using similitude analysis (Kline 1965) for inert constituents, the underlying assumption is that four dimensionless groups characterize the hydrodynamic behavior of fluidized beds. Keeping these constant assures similarity of the flow in the actual and scaled-down apparatus.

The dimensionless groups suggested (Romero and Johanson 1962; Glicksman 1984) are

$$Fr = U^2/gD, \quad \rho_f/\rho, \quad D/d, \quad Re = U\rho_f d/\mu , \tag{83}$$

where, as usual, D is the bed diameter and Fr the Froude number. The bed height is geometrically scaled. The boundary conditions bring in an additional parameter, $p/(\rho_s U^2)$, where p is the pressure at the boundary. With these a flow at atmospheric conditions can be used to model a fluidized, high-temperature combustor bed. For example, it could be used to model a fluidized bed combustor with a gas density of 0.5 kg/m^3 consisting of particles of a

density of 2,600 kg/m^3, a diameter of 1,000 μm, and a gas viscosity of 4.5×10^{-5} kg/(m-s), a model using air at 1.2 kg/m^3, gas viscosity of 1.9×10^{-5} kg/(m-s) and particle density of

$$\rho_{s,c} = \rho_{s,h}\rho_{f,c}/\rho_{f,h} , \tag{84}$$

(i.e., a value of 6.24 kg/m^3). With the Reynolds and Froude numbers constant, the size of the cold bed is only one third that of the modeled hot bed.

Experimental confirmation of the validity of this approach has been obtained by several authors including Fitzgerald and Crane (1980). Further credence of the similarity is obtained by measuring the spectral density of the pressure fluctuations in the two beds. Similarity of the spectra assures hydrodynamic similarity.

It is noteworthy that the ballistic literature does not contain citations where scaling laws and cold flow experiments of fluidized beds have been used to predict behavior of combusting beds. In this case, additional parameters enter into the analysis as we show in a forthcoming publication.

3. MODELS IN VOGUE

The models described in the previous sections have been refined and extended by a number of researchers and form the basis of current calculations of propellant bed drag. A summary of these is given in Tables 4a and 4b. We note that, following Ergun (1952), two friction factors, f_k and f_v (also denoted as *Fk* and *Fv*, respectively), are in use. This first is

$$f_k = (\Delta p/L)\, d_p/(\rho U^2)\varepsilon^3/(1-\varepsilon) , \tag{85}$$

and the second,

$$f_v = (\Delta p/L)\, d_p^2/(\mu U_m)\varepsilon^3/(1-\varepsilon)^2 . \tag{86}$$

It is noteworthy that f_k contains U^2 while f_v contains d_p^2. f_v expresses the ratio of the pressure drop to the viscous energy term while f_k is the total energy loss to the kinetic energy losses. Values of f_v increase with increasing $Re/(1 - \varepsilon)$ from 150 into the thousands while f_k goes from several hundred at a $Re/(1 - \varepsilon)$ value of 1 to around 1.75 for the modified Reynolds number of several thousand. The total energy loss in the bed is the sum of both viscous and kinetic energy losses but, depending on the *Re* number regime, one or the other may predominate. Representative curves of f_k and f_v are shown in Figures 1 and 2.

The Reynolds number in this tabulation has been divided by $1 - \varepsilon$, except for the data of Barth and Esser (1933). Note that in Tables 4a and 4b, we use the generic f to simplify the notation. In all of these models there is a heavy reliance on Ergun's model. Consequently, the limits of validity are circumscribed by his physical assumptions. For example, the pipe-to-particle diameter ratio does not appear in the formulas; thus, the effect of the proximity of the walls is not directly included. Several other points should be noted: Validity of the correlations are restricted to the indicated *Re* number and porosity regimes. Extrapolation of the formulas to outside these regimes usually entails a serious error; for later in the ballistic cycle (i.e., when the projectile has travelled some distance), the physics of the flow is different and consequently this should be reflected in the correlations employed.

4. CRITIQUE OF CURRENT ORTHODOXY

The methods outlined, and in current use, have been criticized on several accounts. Molerus (1980) argues that the bundled tube approach is inconsistent since as $\varepsilon \rightarrow 1$, a limiting resistance for a single particle is not predicted. Also, objections to the submerged object approach have been voiced on the basis that it predicts too small of a pressure drop dependence on volumetric particle concentrations. None of these criticisms has been answered in a satisfactory manner.

4.1 Improved Versions of the Ergun Model. Considerable literature exists on attempts to extend Ergun's equation to higher Reynolds numbers, porosities, and fluidized bed conditions. Recall that the friction factor can be expressed as

$$f = 36[C_1(1 - \varepsilon)]/Re + C_2 , \qquad (87)$$

Table 4a. Summary of Models in Vogue

Reference	Coefficient of Drag, Fk	Shape	Reynolds No./ Void Regime
Ergun (1952)	$f = 150/Re + 1.75$	various	$0.67 < Re < 2{,}300$ $0.4 < \varepsilon < 0.65$
Brauer (1960)	$f = 160/Re + 3.1/Re^{0.1}$	spheres	$2 < Re < 20{,}000$ $0.331 < \varepsilon < 0.681$
Reichelt (1972)	$f = 150/Re + 1.3$ $f = 200/Re + 1.56$	spheres cylinders	$0.2 < Re < 30{,}000$ $0.34 < \varepsilon < 0.41$
Tallmadge (1970)	$f = 150/Re + 4.2/(Re)^{0.16}$	spheres	$0.1 < Re < 10{,}000$ $0.35 < \varepsilon < 0.88$
Wentz and Thodos (1963)	$f = 0.351/(Re^{0.05} - 1.20)$	spheres cylinders	$2{,}550 < Re < 64{,}900$ $0.354 < \varepsilon < 0.882$
Barth and Esser (1933)	$f = 490/Re + 100(Re)^{-0.5} + 5.85$	spheres	$0.1 < Re < 100{,}000$ $0.48 < \varepsilon < 0.62$

Table 4b. Summary of Models in Vogue

Reference	Coefficient of Drag, Fv	Shape	Reynolds No./ Void Regime
Ergun (1952)	$f = 150 + 1.75Re$	various	$0.67 < Re < 2{,}300$ $0.4 < \varepsilon < 0.65$
Kuo and Nydegger (1978)	$f = 276.23 + 5.05(Re)^{0.87}$	spheres	$767 < Re < 24{,}330$ $0.37 < \varepsilon < 0.39$
Robbins and Gough (1978)[a]	$f = 2.50Re^{-0.081}\lambda^{2.17}$	spheres cylinders	$Re < 121{,}675$ $0.396 < \varepsilon < 0.509$
Jones and Krier (1983)	$f = 150 + 3.89(Re)^{0.87}$	spheres	$737 < Re < 126{,}670$ $0.38 < \varepsilon < 0.44$

[a] These authors use an inverse drag coefficient f_s and not f_v, where λ is a shape factor, where f_s and f_v differ by the multiplicative modified Re number. However, as Jones and Krier (1983) claim, this data can be shown to follow the form $f = 150/Re + 3.89(Re)^{0.13}$. The form follows from the definition of F_v and setting it equal to the correlation of Jones and Krier and backing out the definition of the inverse drag coefficient. Both forms give similar drag values as shown in Figure 2.

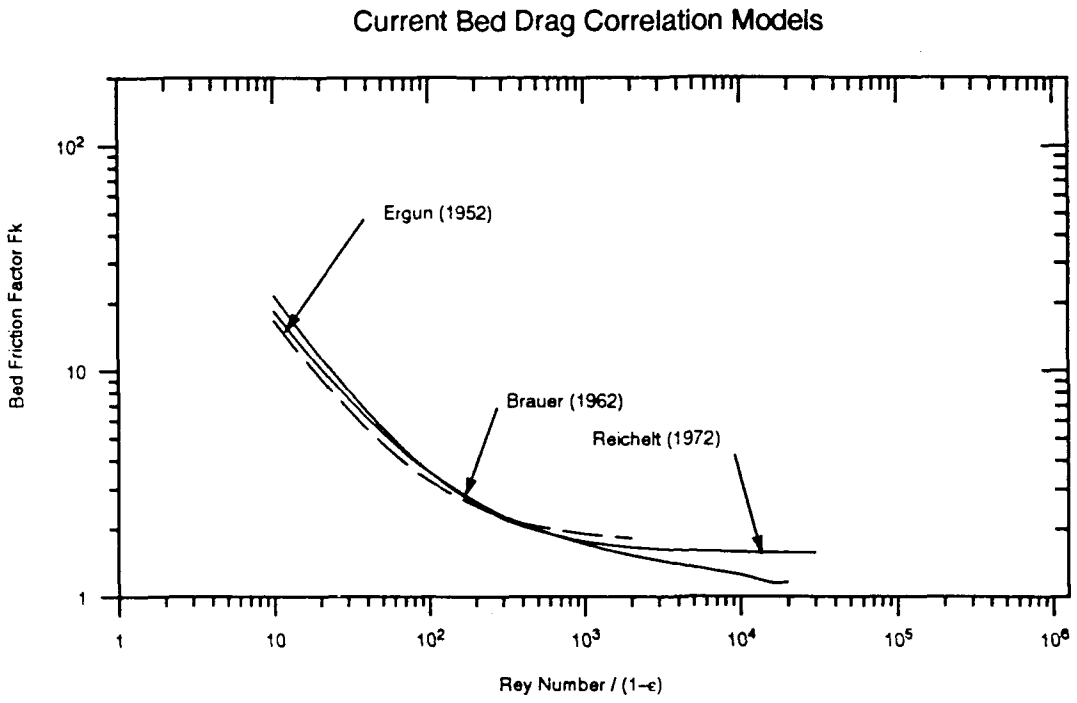

Figure 1. Friction Factor As a Function of Reynolds Number.

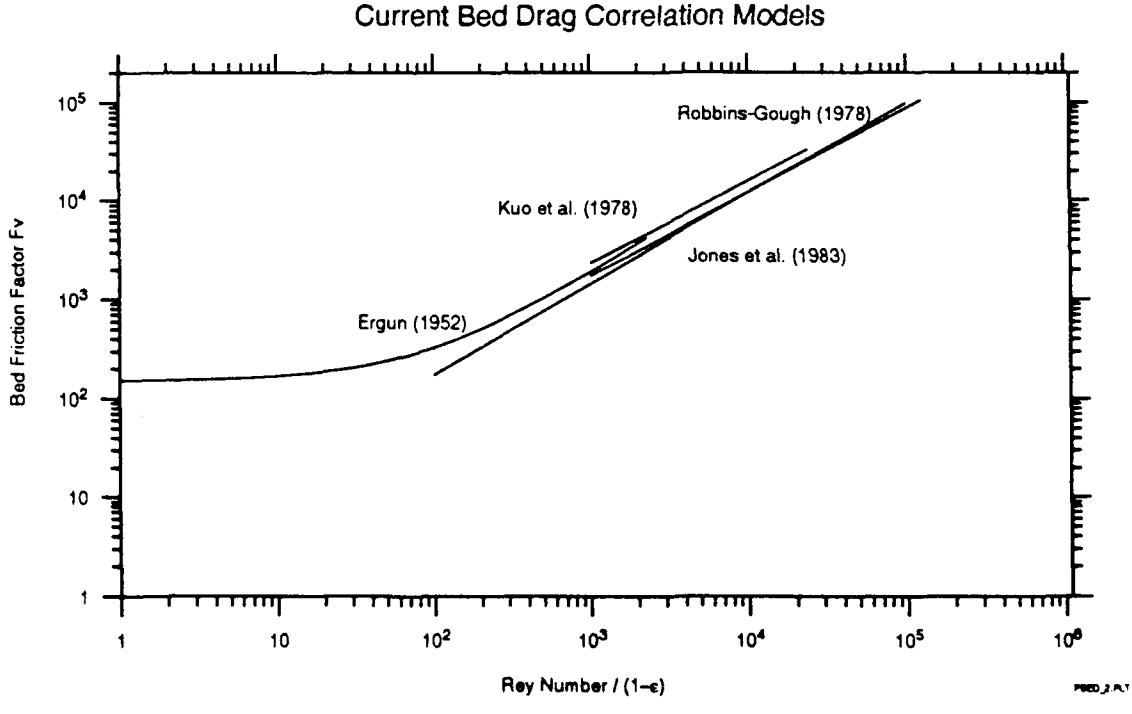

Figure 2. Friction Factor As a Function of Reynolds Number.

where C_1 and C_2 are constants. Along these lines, Tallmadge (1970) suggests

$$f = 150/Re + 4.2/Re^{1/6} . \tag{88}$$

The relationship is valid for spheres in the range $0.1 < Re < 10^5$.

In addition, these theories rely on the assumption that the Kozeny porosity function, $(1 - \varepsilon)^2/\varepsilon^3$, can be treated as a constant. Some have assumed that

$$C_1 = k_o q^2 , \tag{89}$$

where q is the tortuosity factor (i.e., the quotient of the equivalent to the actual channel length) (Carman 1956) and k_o is a shape factor. There is some evidence from experimental data that C_1 should be higher if the Kozeny porosity factor is to be retained. Andersson (1961) suggested a modification of the hydraulic radius approach to take account of higher porosities by the introduction of a factor which depends on the shape of the channel cross section perpendicular to the direction of the flow and also on the porosity. His pressure drop equation then looks as follows:

$$\Delta P/L = zq^2 [\mu U/\varepsilon R_h^2] + C_i q^3 [\rho U^2/R_h^2 \varepsilon^2] , \tag{90}$$

where zq^2 is the Kozeny factor, usually determined from pressure drop measurements in the viscous flow regime; C_i the inertial drag coefficient; and $C_i q^3$ from the fully turbulent flow regime.

The packing geometry determines the passage available for the gases. As Molerus (1980) has pointed out, considerable difference in the volume available is encountered among the packing schemes.

4.2 Shortcomings of the Theoretical Models. An examination of the currently used models reveals that, at least in the ballistic context, some of the assumptions on the nature of the flow are not met and this may contribute to the discrepancy between the observed flow

and the model prediction. The Ergun model, the mother of all ballistic drag models, is based on the assumption of steady gas flow through a stationary bed. Typically, this does not hold true. In addition, and maybe more importantly, the models in vogue leave out several aspects of the physical processes thought to take place in the bed. The fine thread which runs through these observations is, first, that the transient nature of the flow is unaccounted for, and second, as soon as the ignition stimulus is present, gas evolution commences and with it the bed drag changes. This too has been disregarded. Specifically,

1. Propellant gases are generated as the igniter works its way through the bed. No account has been taken of the added mass generation on the drag and especially the change in losses in response to this process.

2. In an actual ballistic situation, gas generation takes place within the bed, thus, it is likely that the gas velocity will deviate from the steady values assumed in the models and simulated in the experiments.

3. The gases from the igniter spread from a localized region and not uniformly across the whole cross section as the ignition process starts. Also, there is some evidence that gases may reflect back off the base of the projectile before the latter begins to move.

4. Hand in hand with the ignition process, of course, goes the change in void fraction as the propellant is consumed. This process is unsteady, but the unsteadiness is unaccounted for in any of the drag theories used for propellant bed drag determination.

5. Many of Ergun's epigones assumed sphericity of the particles making up the bed. Deductions from such flows are not directly applicable to the ballistic situation.

6. A corollary of this is the sensitivity of the model predictions to the value of the $(1 - \varepsilon)$ factor in the equations. A small error in ε will have a big effect on the bed drag.

7. For $D/d_p < 40$ (most ballistic problems fall within this regime), wall effects can have a large influence upon the bed drag force.

8. The models used assume a uniform voidage distribution throughout each cross section. Experimental evidence exists in the chemical literature that this is an idealization and needs to be examined.

9. In some ballistic configurations, a large center void exists due to the presence of an igniter or other geometrical requirements. Although some models make provisions for this, experimental data is nonexistent on bed drag in this situation and, therefore, model validation is difficult to achieve. Interestingly enough, the bubbling phase of a fluidized bed is analogous to this flow in many respects.

10. There is scant evidence to suggest that the Ergun type of formulation retains its validity into fluidized regime. Bed drag, once the bed is in motion, needs more scrutiny. Also, the theory does not account for the axial velocity changes through the bed.

11. When particles are in close proximity, their flow fields influence each other. Since particle drag value, as well as heat transfer coefficients, can be extrapolated from a single to a group of particles without incurring an error which may be hard to quantify.

12. Stick propellant drag is only incompletely understood at the present time.

13. Criteria for fluidization, i.e., dispersion in the phraseology of P. Gough, of a propellant bed need to be reexamined.

14. Some two-phase flow models are based on averaged fluid properties. It is known that the viscosity of a fluidized bed deviates from that of the working fluid. For small shear stresses, the fluidized bed behaves as a Newtonian fluid, but the viscosity has a high value at fluidization, falling with increase in gas velocity.

Generally, the viscosity increases with the size of the particles. Current flow models do not account for these effects.

15. An analysis of the scaling relationships for fluidized, reacting propellant beds has not been performed.

16. Other approaches, such as statistical packed-bed descriptions (Scheidegger 1974), or the use of chaos (Singh and Joseph 1990) have, as of this date, yielded inconclusive results.

Much of the data from the chemical process literature refers to flows at fairly low Reynolds numbers, but there are exceptions (i.e., Davidson, Clift, and Harrison [1985]). Of course, in the stationary packed-bed, flow velocities are also moderate. Viscosity plays a more central role here than later, when fluidization starts. Still, many of these models can be modified for adoption of ballistic flows.

4.3 Bed Experiments. The progress in instrumentation technology over the past decade has not yet percolated down to the measurement of parameters of the packed and fluidized beds. What scarce data are available (Table 5) rely on traditional pressure measurements in stationary, inert beds at low pressures. At best, these are only representative of the initial moments of the ballistic cycle and certainly cannot give insight into actual bed behavior over time. But does it really matter? Skeptics will point to the accuracy of pressure predictions of hydrocodes and, indeed, much progress has been achieved without an accurate depiction of the transient, reactive hydrodynamics of propellant beds. But we have reached the limits of these approaches—further progress depends on a better understanding and simulation of the actual processes within the bed. Table 5 gives the experimental conditions under which available packed-bed measurements were performed with an eye toward replicating ballistic conditions.

The test sections in these experiments consisted of cylindrical tubes preceded by a plenum chamber with straightening vanes to smooth the airflow. A screen mesh or a similar device to restrain the movement of the particles was used to secure the bed material. Orifice

Table 5. Experimental Conditions of Available Packed-Bed Measurements

Reference	Bed Diameter (cm)	Test Section Length (cm)	Particle Scale (cm)	D/d_p	P_{max} (MPa)	Remarks
Ergun (1952)	2.54	20.0	0.02–0.10	25–111		glass, lead shot
Kuo and Nydegger (1978)	0.77	30.0	0.0826	9.3	14.0	WC 870 ball
Robbins and Gough (1978)	7.62	93.0	1.39–30.3	9.6–60	20.0	perf
Jones and Krier (1983)	2.54–5.08	20.3	0.96–6.0	8.5–50	2.5	glass beads

meters and sonic nozzles were employed to measure the mass flow and thermocouples to monitor the temperature within the bed. Air or other gases, such as nitrogen, was let through the bed and the pressure drop monitored at several stations along the test section. The data obtained then were fit by least squares to a model, such as

$$f = aRe^n + b \ . \tag{91}$$

4.4 The Missing Data Syndrome. Despite the progress achieved, data on the following, both for the packed and fluidized beds cases are lacking:

1. Beds with a center core void. Annular, two-phase flow measurements would lend some needed insight.

2. Assessment of the effect of the proximity of the wall.

3. Robbins and Gough (1978) measured bed drag for some propellants with and without perforations. More experimental data is needed on a variety of propellant configurations.

4. Measurement of void distribution across the bed.

5. It is not at all certain that the pressure measured at the wall is representative of the distribution across the tube. Since we know that the void fraction in the radial direction is variable, the difference in response of the gages to the particles and the gas especially need to be examined (Campbell and Wang 1991).

6. Analogously for the value of the gas flow. The distribution of the flow velocity in a cross section downstream of the bed is lacking. The use of bulk flow velocity leads to errors in the drag value.

7. The difficulty and the expense involved in running fixed-bed experiments at elevated Reynolds numbers prevent the performance of many validation checks. For example, how steady is the flow through the bed when the data is taken? This is of importance when one considers the dependence of particle drag on the flow acceleration.

8. Aside from pressure measurements, no ballistic fluidized bed data is available. This includes data on the relative velocity of the phases as a function of radial and axial positions.

9. Except for the Mark II measurements in Whitelaw's group at Imperial College (Bicen, Kliafas, and Whitelaw 1986), boundary layer measurements in fluidized beds of interest to ballisticians are not available.

10. All the data taken are at ε = constant, while in the propellant bed there is an axial dependence.

The data in the fluidized bed literature is mainly concentrated in the lower Reynolds number regimes. Such data has to be used with caution for ballistic modeling. However, this does not negate or lessen the insights which can be gleaned from learning the nature and peculiarities of these flows. Indeed, a knowledge of these cases is a prerequisite for the planning of experimental investigations of the propellant bed.

4.5 Some Shortcomings of the Experimental Data in the Literature. With the notable exception of Jones and Krier (1983), most of the data reported in the literature lack error estimates. Thus, an assessment of the validity of the reported values is difficult at best. This is especially true for the void fraction, which has an overriding importance on the accuracy of the predicted losses. Although the use of a hydraulic radius is an improvement over the conventional channel radii, good estimates of the actual channel lengths in packed-beds are unavailable. Bends in the flow channels can have significant effects on the losses. The same comment applies to changes in the area open to the flow, especially since it is known that the porosity near the wall can be quite different from that elsewhere in the bed. Finally, the flow, especially in the ballistic context, is turbulent. The level and nature of turbulence present has not been measured. The measurement of two-phase flow turbulence is in its infancy.

Overall, theory and experiment show wide discrepancies. The Ergun relationship can represent observations only within ±30% of most measurements. There are also some questions on the reproducibility and, thus, the accuracy of the experimental data due to the observed scatter in the reported values.

5. IMPROVED DRAG RESISTANCE MODELS

5.1 Overview. From the previous chapters, we see that, basically, there are two approaches to describing the flow resistance in a porous medium. In the first, without regard to the physics, equations are heuristically fit to available experimental data so as to relate the pressure drop through the bed to the velocity. Fixed bed experimental data (i.e., pressure drop through a bed with the gas velocity constant) is converted to drag correlations relating pressure (i.e., friction factor) to porosity and Reynolds number. Forchheimer (1901) proposed this scheme by modifying Darcy's law.

This semi-theoretical reasoning has led to a large number of drag relations including Ergun's equation. While this approach has been useful, it does not further our physical understanding of the flow. Also, note that the experiments rely on the fact that the void fraction is the same through the bed—in the real situation, ε varies both axially and radially.

A refinement of the existing models is possible if one considers the transient nature of the flow, and effect of the gas generation process taking place in the interstices of the bed. The overall effect can be reduced to several observables which include:

(a) gas generation, effect of mass generation on the drag
(b) effect of the unsteadiness of the flow on the drag prediction

There are two subsidiary questions here. First, how is the friction factor affected by the unsteadiness of the flow and, secondly, how does the unsteadiness affect the pressure loss through the bed?

5.2 Effect of Mass Transfer in the Flow on the Drag. When mass transfer is taken into account, an improved drag model of the bed is obtained. Toward these ends, several approaches come to mind—the simplest modifies the frictional drag coefficient by taking account of the mass generation left out of current bed drag correlations. Picture a bed made up of spheres which undergo a phase change, prior to combustion, analogously to that of a liquid droplet. Then, using Equation 64 instead of one of the relations from Table 2, the Ergun relationship yields the following friction factor for the bed,

$$f = 0.75[(1/(1+B)^{0.2}](24/Re)(1+0.2Re^{0.63})\varepsilon^3 \ . \qquad (92)$$

Substituting values for air and comparing with inert flow, one sees immediately that the presence of mass transfer will have noticeable effect on the friction factor of the bed. Equation 64 was derived for low Reynolds number flows, but a sizeable literature exists on drag coefficients in the presence of mass transfer at high Reynolds numbers (i.e., ablating surface flows).

The effect can be quite noticeable. For example, at $Re = 10^3$, $f = 0.026$, but, if $B = 0$, $f = 0.3$, the value usually used in code calculations.

This approach, of course, is still inadequate in the sense that the model only addresses the low Reynolds number regime. At higher Reynolds numbers, the flow and mass transfer equations must be solved simultaneously to get the effect of the mass transfer on the value of

the friction factor (Watson and Balasubramanian 1984). The model then consists of a steady, initially incompressible convective flow over a surface, which due, to the heating from the gas flow, reacts in an infinitely thin layer. The reaction products are carried into the flow. Due to their presence, the velocity distribution and, consequently, the shear stress on the bounding surface is altered resulting in a change in the friction factor.

The flow among the propellant grains in characterized by the constant change in direction of the gas as it threads its way through the propellant aggregate. It has many commonalities with flow over a corrugated surface. The size of the particles, as well as the packing geometry, accounts for the similarity to the periodicity or waviness of the surface as well as the corrugation wave amplitude. The effect of combustion on the velocity profile can be simulated by making the corrugated surface porous allowing the injection of mass into the convection stream. The exothermicity is accounted for by varying the specific heat and the temperature of the injected mass. (See Figure 3.)

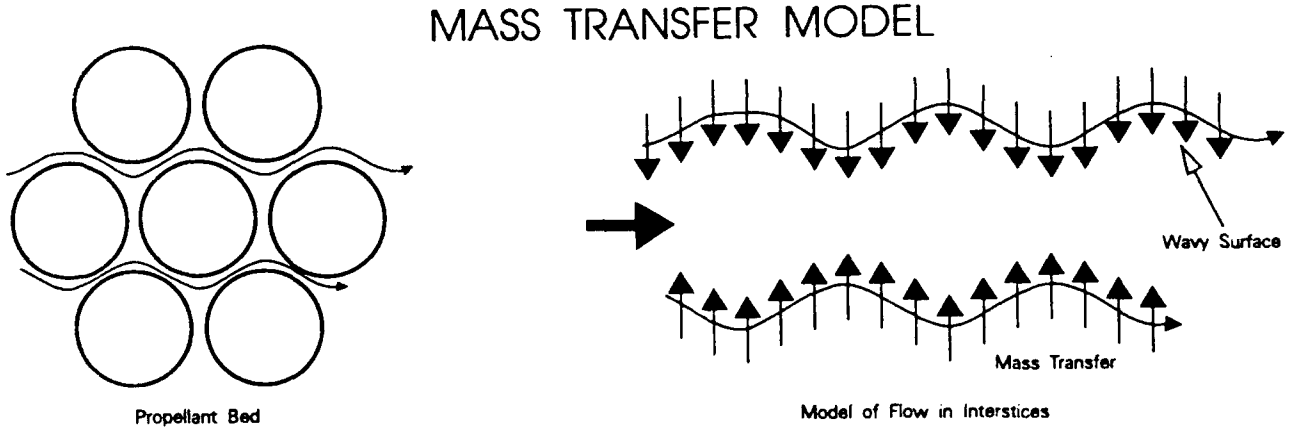

Figure 3. Model of the Ablating Propellant Bed.

The proposed algorithm is as follows:

1. Calculate the velocity distribution in the turbulent boundary layer.
2. Obtain the shear stress relationship.

3. Integrate the viscous stress over the surface.
4. Compare with the single component expression (i.e.,where no mass transfer takes place in a smooth tube).

One of the important parameters is the exothermicity of the reaction which has a great influence on the flow profile.

5.3 Effect of Unsteadiness on the Drag Correlation. There does not exist an unequivocal answer to the question to what extent value of the friction factor, *f*, changes in an unsteady flow. Generally, it is thought to be lower than the steady state value. The question is an important one, since in interior ballistic code calculations, at each point in the calculational grid (i.e., position in the gun tube) a value of *f* is chosen reflecting the porosity and *Re* number. The *f* values are taken from steady-state experiments. Since the hydro-code itself includes the time dependent terms, it is assumed implicitly that this will take care of the effect of unsteadiness on the friction factor also. Thus, an improved approach is to derive and/or measure a friction factor for unsteady flow and use these unsteady values in the code calculations. We believe the latter approach mimics and models the actual physics better and gives a derivation based on an unsteady formulation.

Friction factor under unsteady flow conditions has been studied by a number of authors (Wood and Kao 1968; Iguchi and Ohmi 1983; Kovetskaya, Platonov, and Laurik 1987). To gage the effect of unsteadiness on the friction factor, the preferred approach has been to study oscillating flow fields and measure the shear stress on the walls of the container. Other attempts, such as those of Goodwin (1986), were to gauge the change in *f* when a step change in discharge occurs in a river carrying sediment. A slight decrease in friction factor was reported.

The heuristic argument of Ergun relies on the fact that the pressure drop through the bed is proportional to *U*. However, in the early part of the ballistic cycle, as the primer gas rushes through the fixed bed, the gas experiences considerable acceleration. In fact, from computer simulation of a 120-mm gun firing (Robbins 1991), when the gas velocity is 70 m/s, the acceleration is typically around 10^4. By a simple order of magnitude analysis, it can be shown that the acceleration term is of the order or larger than the convective term.

Forchheimer (1901) appears to have been the first one to have suggested that the pressure drop through an aggregate may be proportional not only to the first and second powers of the velocity but also to higher powers. Theories built around this concept though have not gained many adherents.

Same holds for adding a time derivative term. Both Polubarinova-Kochina (1962) and Irmay (1958) briefly allude to it, but claim that this term is negligible. That is probably correct for seepage through soil, which was their main concern. Consideration was also given to the Bassett-Boussinesq-Oseen equation (Gough 1974), for example, to assess the effect of the presence of virtual mass and acceleration of small particles on the force balance. This approach though relies on several assumptions which are no longer met in the situation of interest here, see also Draw et al. (1979).

In the ballistic context, of course, the changes in the velocity through the propellant bed are substantial. Thus, as shown below, one needs to consider the pressure drop through the bed to be

$$\Delta p/L = aU + bU^2 + c\rho U_t \,, \tag{93}$$

where U_t, the new term, is the gradient in the velocity and the coefficient c is inversely proportional to the void fraction. This term can under may circumstances be of the same order as the second term and will contribute to the pressure drop. Certainly, it should not be neglected.

Recall that earlier, *Fv* was defined as

$$Fv = \frac{\Delta p}{L}\frac{d_p^2}{\mu U}\frac{\varepsilon^3}{(1-\varepsilon)^2} = k_1 + k_2\frac{Re}{1-\varepsilon} \,, \tag{94}$$

where to coefficients were determined by least squares fitting of the data.

In the presence of unsteadiness, the last term on the right of Equation 93 then has to be multiplied by the factor which multiplies the $\Delta p/L$ in Equation 94. Thus, the expression for Fv, at a particular Re, becomes,

$$Fv = a + b(Re^{c}) + d\left[\frac{\varepsilon^2}{(1-\varepsilon)^2}\right]\left[\frac{\rho^2 d^3}{\mu^2}\right]\frac{1}{Re}U_t\,, \tag{95}$$

where U_t is the acceleration. The coefficients are determined by nonlinear regression. The data of Jones and Krier (1983), which is fairly representative of the available flow measurements, when modified for an acceleration of 10^4, yielded the following correlation coefficients: $a = -774.24$, $b = 4.73$, $c = 0.85$, and $d = 277.60$. This then is one possible form of the new zeroth order model of the bed drag and can be interpreted as giving a qualitative idea of the trends expected when acceleration is included. Experiments under unsteady conditions will have to be performed, such as the one currently planned at BRL, to determine the exact correlation coefficients when acceleration is present.

It is important to emphasize the assumptions of the model: (1) effects are additive as it is implicit in both the Forchheimer and the Ergun models and (2) the pressure drop is proportional to U, U^2, and U_t. Due to the unavailability of reliable measurements, the magnitude of the acceleration was obtained from interior ballistic simulations.

Figure 4 shows the bed drag, Fv, both for the conventional as well as the proposed models. Though under ballistic conditions, the gases through the bed accelerate, both Kuo and Nydegger (1978) and Jones and Krier (1983) investigated bed drag under steady-state conditions. The proposed model makes provisions for the acceleration of the gases which is observed after the inception of the ballistic cycle. The estimate of the acceleration was taken from Robbins (1991) for a typical gun firing. The precise magnitudes of the accelerations, of course, depend on the specifics of the charge, but the trends are unmistakable. At low to medium Reynolds numbers, the accelerations are important for the drag magnitude. Past $Re = 10^5$, the acceleration becomes less important and is overshadowed by other effects contributing to bed drag. Thus, it is reasonable to postulate that the contribution to bed drag of the unsteadiness in the velocity in the early part of the ballistic cycle is important and can

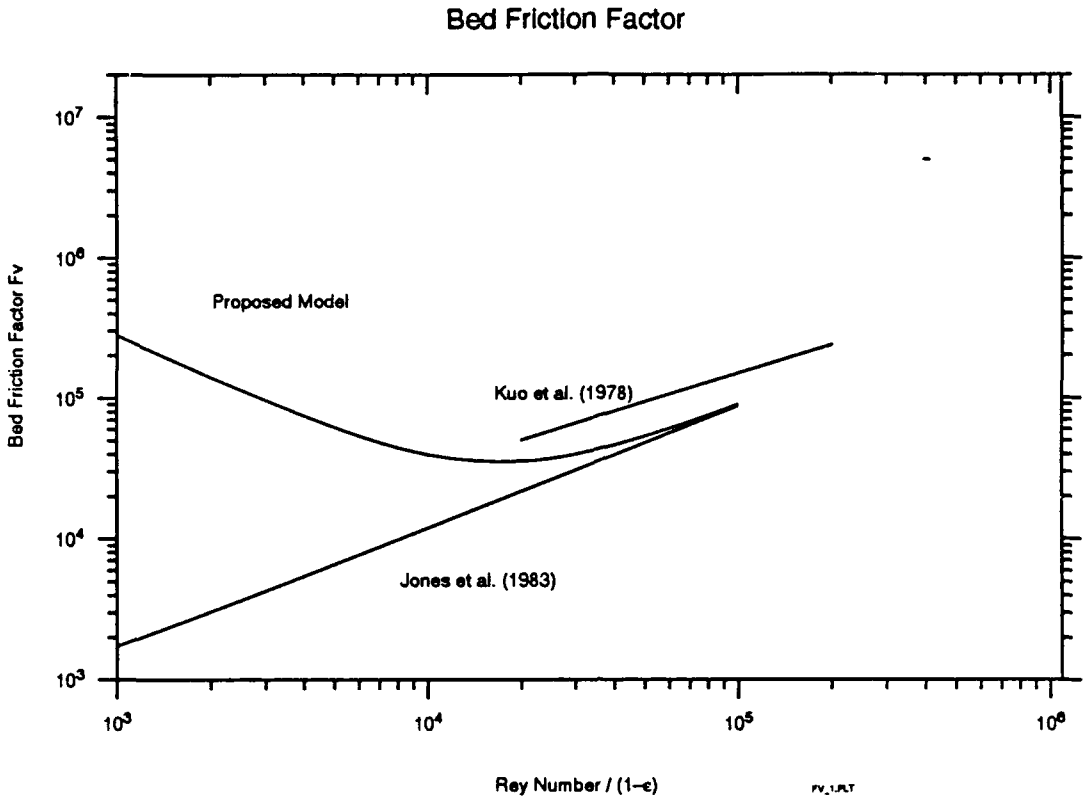

Figure 4. Coefficient of Drag As a Function of Reynolds Number.

not be neglected without incurring an error in the bed drag determination. Subject to further refinement and the availability of acceleration data, the proposed model at present should be interpreted as showing trends and not absolute drag values.

6. DISCUSSION

Based on engineering estimates, the values of the parameters which control the global behavior of packed beds used in the chemical process industry can be predicted, especially at low Reynolds numbers, with considerable assurance.

Packed beds in guns have many commonalities with conventional packed beds, but there are also some differences. Notable among these is that fluidization in the ballistic case starts from gas generation within the bed instead of flow from without. Thus, chemical packed bed models and correlations must be used with caution in the ballistic case.

To gain further insight into the microflow behavior of propellant packed and fluidized beds, an approach based on first principles, possibly probabilistic (i.e., statistical in nature), need to be considered. Such calculations tend to be cpu time intensive but with the availability of massively parallel computers these calculations are now economically possible.

7. CONCLUSIONS

Considerable progress in quantifying bed drag has been made since Osborne Reynolds, around the turn of the century, showed that the pressure drag of a granular bed is proportional to the velocity of the gas flow through it. After examining the literature, and far from engaging in floccinaucinihilipilification,* it was found that the models in use today to predict bed and fluidized drag are open to criticism on several accounts. These have been discussed in detail. Most importantly, physics left out of the models needs to be included. Suggestion for an approach and outlines of two improved drag models have been presented. From these, the lessons learned include two salient points. One, that the bed drag, fluidized or stationary, will vary substantially depending on whether mass transfer from the grains is allowed and secondly, the gas acceleration can and does have an important bearing on the magnitude of the bed drag during the early part of the ballistic cycle. It has also been shown that the chemical process literature contains a wealth of data on fluidized beds, information which though not directly transferable to the propellant bed, can serve as useful guideposts for elucidating unknown facets of the bed flow dynamics.

In addition, the need for considerably more experimental data, both of the stationary as well as the moving bed, for many configurations of interest today (i.e., the unicharge) has been demonstrated. This is a challenging undertaking but then, fortes fortuna juvat (fortune favors the brave).

---

* action or habit of estimating as worthless, Oxford English Dictionary, First Ed.

INTENTIONALLY LEFT BLANK.

8. REFERENCES

Achenbach, E. "The Effect of Surface Roughness and Tunnel Blockage on the Flow Past Spheres." Journal of Fluid Mechanics, vol. 65, pp. 113–125, 1974.

Allen, T. Particle Size Measurement. 3rd ed., London: Chapman Hall, 1981.

Andersson, K. E. B. "Pressure Drop in Ideal Fluidization." Chemical Engineering Science, vol. 15, pp. 276–297, 1961.

Barth, W., and W. Esser. "Der Druckverlust in Geschichteten Stoffen". Forschung, vol. 4, pp. 82–86, 1933.

Benenati, R. F., and C. B. Brosilow. "Void Fraction Distribution in Beds of Spheres." AIChE Journal, vol. 8, pp. 359–361, 1962.

Bicen, A. F., Y. Kliafas, and J. H. Whitelaw. "In-Bore Velocity Measurement in the Wake of a Subsonic Projectile." AIAA Journal, vol. 24, pp. 1035–1037, 1986.

Bird, R., W. Stewart, and E. Lightfoot. Transport Phenomena. New York: Wiley, 1966.

Brauer, H. "Eigenschaften der Zweiphasen-Stroemung bei der Rektifikation in Fullkorpersaulen." Dechema-Monographien, Bd. 37, Verlag Chemie GmbH, 1960.

Campbell, C. S., and D. G. Wang. "Particle Pressures in Gas-Fluidized Bed." Journal of Fluid Mechanics, vol. 227, pp. 495–508, 1991.

Carman, P. C. Flow of Gases Through Porous Media. New York: Academic Press, 1956.

Chalmers, J., D. B. Taliaferro, and E. L. Rawlins. "Flow of Air and Gas Through Porous Media." Trans. AIME, vol. 98, p. 375, 1932.

Clift, R., J. R. Grace, and M. E. Weber. Bubbles, Drops, and Particles. New York: Academic Press, 1978.

Davidson, J. F., R. Clift, D. Harrison. Fluidization. 2nd. ed., London: Academic Press, 1985.

Drew, D., L. Chang, R. T. Lahey. "The Analysis of Virtual Mass Effects in Two-Phase-Flow." International Journal of Multiphase Flow, vol. 5, pp. 233–242, 1979.

Eisenklam, P., S. A. Arunachalan, and J. A. Weston. "Evaporation Rates and Drag Resistance of Burning Drop." Eleventh International Symposium of Combustion, Combustion Institute, Pittsburgh, PA, pp. 715–727, 1967.

El-Kaissy, M. M., and G. M. Homsy. "A Theoretical Study of Pressure Drop and Transport in Packed Beds at Intermediate Reynolds Numbers." Industrial Engineering Chemical Fundamentals, vol. 12, pp. 82–90, 1973.

Emmons, H. W. "The Film Combustion of Liquid Fuel." Z. Angew. Math. Mechanik, vol. 36, pp. 60–71, 1956.

Epstein, N., and S. Levine. "Non-Darcy Flow and Pressure Distribution in a Spouted Bed." Fluidization. J. F. Davidson, D. L. Keairns, editors, London: Cambridge University Press, 1978.

Ergun, S. "Fluid Flow Through Packed Columns." Chemical Engineering Progress, vol. 48, pp. 89–94, 1952.

Fayon, A. M., and J. Happel. "Effect of a Cylindrical Boundary on a Fixed Rigid Sphere in a Moving Viscous Fluid." AIChE Journal, vol. 6, pp. 55–58, 1960.

Fitzgerald, T. J., and S. D. Crane. Proceedings of the International Conference of Fluidized Bed Combustion. Vol. III, No. 6, pp. 815–820, 1980.

Fond, R. M., and R. Thinakaran. "The Influence of the Wall on Flow Through Pipes Packed With Spheres." Trans. ASME, Journal of Fluids Engineering, vol. 112, pp. 84–88, 1990.

Forchheimer, P. "Wasserbewegung Durch Boden". Z. VDI, vol. 45, pp. 1782–1788, 1901.

Foscolo, P. U., and L. G. Gibrilaro. "A Fully Predictive Criterion for the Transition Between Particulate and Aggregate Fluidization." Chemical Engineering Science, vol. 39, pp. 1667–1675, 1984.

Foumeny, E. A, and S. Roshani. "Mean Voidage of Packed Beds of Cylindrical Particles." Chemical Engineering Science, vol. 46, pp. 2363–2364, 1991.

Geankoplis, C. J. Transport Processes: Momentum, Heat, and Mass. Boston: Allyn and Bacon, Inc., 1983.

Geldart, D. Gas Fluidization Technology. Chichester: John Wiley, 1986.

Glicksman, L. R. "Scaling Relationships for Fluidized Beds." Chemical Engineering Science, vol. 39, pp. 1373–1379, 1984.

Goodwin, P. "Sediment Transport in Unsteady Flows." PhD Thesis, Graduate Division, University of California, Berkeley. Ann Arbor, UMI, 1986.

Gough, P. S. "The Flow of a Compressible Gas Through an Aggregate of Mobile Reacting Particles." PhD Thesis, McGill University, 1974.

Gough, P. S. "Numerical Analysis of a Two-Phase Flow With Explicit Internal Boundaries." Naval Ordnance Station, Indian Head Contract Report 77-5, 1977.

Happel, J. "Viscous Flow in Multiparticle Systems." Slow Motion of Fluids Relative to Beds of Spherical Particles, AIChE Journal, vol. 4, pp. 197–201, 1958.

Hewitt, G. F. "Chemical Engineering in the British Isles: The Academic Sector." Trans. I. Chemical Engineering, vol. 69, pp. 79–90, 1991.

Hinze, J. O. "Momentum and Mechanical-Energy Balance Equations for a Flowing Homogeneous Suspension With Slip Between the Phases." Applied Scientific Research, vol. A11, pp. 33–46, 1961.

Hirata, A., and F. B. Bulos. "Predicting Bed Voidage in Solid-Liquid Fluidization." Journal of Chemical Engineering, Japan, vol. 23, pp. 599–604, 1990.

Howard, J. R. Fluidized Bed Technology. Bristol: Adam Hilger, 1989.

Iguchi, M., and M. Ohmi. "Unsteady Frictional Losses in Decelerating Turbulent Pipe Flows." Technical Report, Osaka University, vol. 33, pp. 349–58, 1983.

Irmay, S. "On the Theoretical Derivation of Darcy and Forchheimer Formulas." Trans. American Geophysical Union, vol. 39, pp. 702–707, 1958.

Jaiswal, A. K., T. Sundararajan, and R. P. Chhabra. "Hydrodynamics of Newtonian Fluid Flow Through Assemblages of Rigid Spherical Particles in Intermediate Reynolds Number Regime." International Journal of Engineering Science, vol. 29, pp. 693–708, 1991.

Jeschar, R. "Druckverlust in Mehrkornschuettungen aus Kugeln." Archiv Eisenhuttenwesen, vol. 35, pp. 91–108, 1964.

Jones, D. P., and H. Krier. "Gas Flow Resistance Measurements Through Packed Beds at High Reynolds Numbers." Journal of Fluids Engineering, Trans. ASME, vol. 105, pp. 168–173, 1983.

Kline, S. J. Similitude and Approximation Theory. New York: McGraw-Hill, 1965.

Kovetskaya, M. M., A. G. Platonov, and V. M. Laurik. "Determination of the Friction Factor of a Fluctuating Gas Flow in a Duct." Fluid Mechanics-Soviet Research, vol. 16, pp. 134–140, 1987.

Kunii, D., and O. Levenspiel. Fluidization Engineering. Malabor, FL: R. E. Krieger Publication Company (reprint), 1969.

Kuo, K. K., and C. C. Nydegger. "Flow Resistance Measurements and Correlation in a Packed Bed of WC 870 Ball Propellants." Journal of Ballistics, vol. 2, pp. 1–25, 1978.

Leung, L. S., and P. J. Jones. "Coexistence of Fluidized Solid Flow and Packed Bed Flow in Standpipes." Fluidization, J. F. Davidson and D. L. Keairns, Eds., London: Cambridge University Press, 1978.

Leva, M. Fluidization. New York: McGraw-Hill, 1959.

Mannsett, T. "On the Fluid-Phase Momentum Balance Laws and Momentum Jump Condition for Porous Media Flow." European Journal of Mechanics B/Fluids, vol. 10, pp. 97–111, 1991.

Mehta, D., and M. C. Hawley. "Wall Effect in Packed Columns." I&EC Proc. Design and Development, vol. 8, pp. 280–282, 1969.

Molerus, O. "A Coherent Representation of Pressure Drop in Fixed Beds and of Bed Expansion for Particulate Fluidized Beds." Chemical Engineering Science, vol. 35, pp. 1331–1340, 1980.

Nishimura, Y., and T. Ishii. "An analysis of Transport Phenomena for Multi-Solid Particle Systems at Higher Reynolds Numbers by a Standard Karman-Pohlhausen Method-I." Chemical Engineering Science., vol. 35, pp. 1195–1204, 1980.

Pike, J. "The Drag of Spheres at Porosities Ranging From an Isolated Sphere to a Packed Bed." Cranfield Institute of Technology, Cranfield CoA Report No. 9012, 1990.

Polubarinova-Kochina, P. Ya. Theory of Ground Water Movement. Princeton, NJ: Princeton University Press, 1962.

Poo, J. Y., and N. Ashgriz. "Variation of Drag Coefficients in an Interacting Drop Stream." Exp. Fluids, vol. 11, pp. 1–8, 1991.

Raju, M. S., and W. A. Sirignano. "Interaction Between Two Vaporizing Droplets in an Intermediate Reynolds Number Flow." Physics of Fluids, vol. A2, pp. 1780–1796, 1990.

Rase, H. F. Fixed-Bed Reactor Design and Diagnostics. Boston: Butterworths, 1990.

Reichelt, W. "Zur Berechnung des Druckverlustes einphasig durchstromter Kugel und Zylinderschuttungen." Chemie Ing. Tech., vol. 44, pp. 1068-1071, 1972.

Renksizbulut, M., and R. J. Haywood. "Transient Droplet Evaporation With Variable Properties and Internal Circulation at Intermediate Reynolds Numbers." International Journal of Multiphase Flow, vol. 14, pp. 189–202, 1988.

Robbins, R. Private communication, U.S. Army Ballistic Research Laboratory, Aberdeen Proving Ground, MD, 1991.

Robbins, R., and P. S. Gough. "Experimental Determination of Flow Resistance in Packed Beds of Gun Propellant." Proceedings of the 15th JANNAF Combustion Meeting, CPIA Pub. 297, 1978.

Roblee, L. H. S., R. M. Baird, and J. W. Tierney. "Radial Porosity Variations in Packed Beds." AIChE Journal, vol. 4, pp. 460–464, 1958.

Romero, J. B., and L. N. Johanson. "Factors Affecting Fluidized Bed Quality." Chem. Eng. Prog. Symp. Ser., vol. 58, pp. 28–37, 1962.

Rowe, P. N. "Drag Forces in a Hydraulic Model of a Fluidized Bed." Part I, II. Trans. Inst. Chem. Eng. London, vol. 39, pp. 41–54 and pp. 175–180, 1961.

Scheidegger, A. E. Physics of Flow Through Porous Media. 3rd ed., Toronto: University of Toronto Press, 1974.

Schwartz, C. E., and J. M. Smith. "Flow Distribution in Packed Beds." Ind. Eng. Chem., vol. 45, pp. 1209–1218, 1953.

Singh, P., and D. D. Joseph. Chaos and Structure in Two-Dimensional Beds of Spheres Fluidized by Water. University of Minnesota Supercomputer Institute Research Report. UMSI 90/44, 1990.

Spalding, D. B. "Mass Transfer in Laminar Flow." Proc. Royal Soc./A221, pp. 78–99, 1954.

Spielman, L., and S. L. Goren. "Model for Predicting Pressure Drop and Filtration Efficiency in Fibrous Media." Environmental Science Technology, vol. 4, pp. 279–287, 1968.

Succi, S., E. Foti, and M. Gramignani. "Flow Through Geometrically Irregular Media With Lattice Gas Automata." Meccanica, vol. 25, pp. 253–257, 1990.

Tallmadge, J. A. "Packed Bed Pressure Drop—An Extension to Higher Reynolds Numbers." AIChE Journal, vol. 16, pp. 1092–1093, 1970.

Tosun, I., and H. Mousa. "Flow Through Packed Beds: Wall Effect on Drag Force." Chem. Engineering Science, vol. 41, pp. 2962–2965, 1986.

Watanabe, H. "Drag Coefficient and Voidage Function on Fluid Flow Through Granular Packed Beds." Institute Journal of Engineering Fluid Mechanics, vol. 2, pp. 93–108, 1989.

Watson, R. D., and R. Balasubramanian. "Wall Mass Transfer and Pressure Gradient Effects on Turbulent Skin Friction." AIAA Journal, vol. 22, pp. 143–145, 1984.

Wen, C. Y., and Y. H. Yu. "Mechanics of Fluidization." Chem. Eng. Prog. Symp. Ser., vol. 62, p. 62, 1966.

Wentz, C. A., and G. Thodos. "Pressure Drops in the Flow of Gases Through Packed and Distended Beds of Spherical Particles." AIChE Journal, vol. 9, pp. 81-84, 1963.

Wood, D. J., and T. Y. Kao. Evaluation of Quasi-Steady Approximation for Viscous Effects in Unsteady, Liquid Pipe Flow. ASME Paper 68-FE-33, New York: American Society of Mechanical Engineers, 1968.

Yoon, S. M., and D. Kunii. "Gas Flow and Pressure Drop Through Moving Beds." I & EC Proc. Design and Development., vol. 9, pp. 559–565, 1970.

Yu, A. B., and N. Standish. "Estimation of the Porosity of Particle Mixture by a Linear-Mixture Packing Model." Ind. Eng. Chem. Res., vol. 30, pp. 1372-1385, 1991.

Yuen, M. C., and L. W. Chen. "On Drag of Evaporating Liquid Droplets." Comb. Sci. Tech., vol. 14, pp. 147–154, 1978.

LIST OF SYMBOLS

A	cross-sectional area
a	constant, filter fiber radius
B	transfer number (Spalding number)
b	constant
C_D	drag coefficient
C_{D^∞}	drag coefficient in unbounded fluid
C_{DS}	drag coefficient of an isolated sphere
c	constant
D	bed diameter
d	particle diameter
d_i	sieve aperture
d_m	mean particle diameter
d_p	particle diameter
d_r	tube to particle diameter ratio
F	drag force
F_D	drag on object in a bounded fluid
F_∞	drag on object in an unbounded fluid
f	friction factor
G_o	mass flow rate
g	acceleration due to gravity
h	hydraulic height
K	wall correction factor
K_F	fractional increase in drag due to presence of walls
K_{ns}	nonspherical correction factor
k	permeability, Darcy coefficient
k_o	shape factor
k_1	coefficient
k_2	coefficient
L	bed length
L	latent heat of vaporization
N	number of particles

n	exponent
n_i	no of particles of size d_i
p	wetted perimeter
p	pressure
Q	flow rate
q	tortuosity factor
R_h	hydraulic radius
S_v	surface area per unit volume
U	velocity
v	velocity in the interstices of the bed
v_o	*superficial velocity*
v_p	volume of solid particle
x	distance
x_i	mass fraction
z	coordinate, cross-section function of Anderson

GREEK

α	constant, volume fraction of fiber
β	constant
δ	boundary layer thickness
ε	void fraction
λ	particle to tube diameter ratio, shape factor
μ	viscosity
ρ	density
σ	stress
τ	shear stress
ϕ	sphericity

SUBSCRIPT

f	fluid
g	gas

i	size range
m	mean
mf	minimum fluidization
ns	nonspherical
p	particle
pk	packed-bed
rz	Richardson-Zaki model
s	surface
sl	slip
sv	surface-volume ratio
t	terminal, also time dependence
w	wall
∞	free stream condition

INTENTIONALLY LEFT BLANK.

No. of Copies	Organization
2	Administrator Defense Technical Info Center ATTN: DTIC-DDA Cameron Station Alexandria, VA 22304-6145
1	Commander U.S. Army Materiel Command ATTN: AMCAM 5001 Eisenhower Ave. Alexandria, VA 22333-0001
1	Commander U.S. Army Laboratory Command ATTN: AMSLC-DL 2800 Powder Mill Rd. Adelphi, MD 20783-1145
2	Commander U.S. Army Armament Research, Development, and Engineering Center ATTN: SMCAR-IMI-I Picatinny Arsenal, NJ 07806-5000
2	Commander U.S. Army Armament Research, Development, and Engineering Center ATTN: SMCAR-TDC Picatinny Arsenal, NJ 07806-5000
1	Director Benet Weapons Laboratory U.S. Army Armament Research, Development, and Engineering Center ATTN: SMCAR-CCB-TL Watervliet, NY 12189-4050
(Unclass. only)1	Commander U.S. Army Rock Island Arsenal ATTN: SMCRI-TL/Technical Library Rock Island, IL 61299-5000
1	Director U.S. Army Aviation Research and Technology Activity ATTN: SAVRT-R (Library) M/S 219-3 Ames Research Center Moffett Field, CA 94035-1000
1	Commander U.S. Army Missile Command ATTN: AMSMI-RD-CS-R (DOC) Redstone Arsenal, AL 35898-5010

No. of Copies	Organization
1	Commander U.S. Army Tank-Automotive Command ATTN: ASQNC-TAC-DIT (Technical Information Center) Warren, MI 48397-5000
1	Director U.S. Army TRADOC Analysis Command ATTN: ATRC-WSR White Sands Missile Range, NM 88002-5502
1	Commandant U.S. Army Field Artillery School ATTN: ATSF-CSI Ft. Sill, OK 73503-5000
(Class. only)1	Commandant U.S. Army Infantry School ATTN: ATSH-CD (Security Mgr.) Fort Benning, GA 31905-5660
(Unclass. only)1	Commandant U.S. Army Infantry School ATTN: ATSH-CD-CSO-OR Fort Benning, GA 31905-5660
1	WL/MNOI Eglin AFB, FL 32542-5000
	Aberdeen Proving Ground
2	Dir, USAMSAA ATTN: AMXSY-D AMXSY-MP, H. Cohen
1	Cdr, USATECOM ATTN: AMSTE-TC
3	Cdr, CRDEC, AMCCOM ATTN: SMCCR-RSP-A SMCCR-MU SMCCR-MSI
1	Dir, VLAMO ATTN: AMSLC-VL-D
10	Dir, USABRL ATTN: SLCBR-DD-T

No. of Copies	Organization
1	Commander U.S. Army Concepts Analysis Agency ATTN: D. Hardison 8120 Woodmont Avenue Bethesda, MD 20014
1	C.I.A. 01R/DB/Standard Washington, DC 20505
1	U.S. Army Ballistic Missile Defense Systems Command Advanced Technology Center P.O. Box 1500 Huntsville, AL 35807-3801
1	Chairman DOD Explosives Safety Board Room 856-C Hoffman Bldg. 1 2461 Eisenhower Avenue Alexandria, VA 22331-0600
1	Commander U.S. Army Materiel Command ATTN: AMCDE-DW 5001 Eisenhower Avenue Alexandria, VA 22333-5001
1	Department of the Army Office of the Product Manager 155mm Howitzer, M109A6, Paladin ATTN: SFAE-AR-HIP-IP, Mr. R. De Kleine Picatinny Arsenal, NJ 07806-5000
2	Commander Production Base Modernization Agency U.S. Army Armament Research, Development, and Engineering Center ATTN: AMSMC-PBM, A. Siklosi AMSMC-PBM-E, L. Laibson Picatinny Arsenal, NJ 07806-5000
3	PEO-Armaments Project Manager Tank Main Armament System ATTN: AMCPM-TMA/K. Russell AMCPM-TMA-105 AMCPM-TMA-120/C. Roller Picatinny Arsenal, NJ 07806-5000
15	Commander U.S. Army Armament Research, Development, and Engineering Center ATTN: SMCAR-AEE SMCAR-AEE-B, A. Beardell D. Downs S. Einstein S. Westley S. Bernstein J. Rutkowski B. Brodman P. O'Reilly R. Cirincione A. Grabowsky P. Hui J. O'Reilly N. DeVries SMCAR-AES, S. Kaplowitz Picatinny Arsenal, NJ 07806-5000
2	Commander U.S. Army Armament Research, Development, and Engineering Center ATTN: SMCAR-CCD, D. Spring SMCAR-CCH-V, C. Mandala Picatinny Arsenal, NJ 07806-5000
1	Commander U.S. Army Armament Research, Development and Engineering Center ATTN: SMCAR-HFM, E. Barrieres Picatinny Arsenal, NJ 07806-5000
1	Commander U.S. Army Armament Research, Development and Engineering Center ATTN: SMCAR-FSA-T, M. Salsbury Picatinny Arsenal, NJ 07806-5000

No. of Copies	Organization
1	Commander, USACECOM R&D Technical Library ATTN: ASQNC-ELC-IS-L-R, Meyer Center Fort Monmouth, NJ 07703-5301
1	Commander U.S. Army Harry Diamond Laboratory ATTN: SLCHD-TA-L 2800 Powder Mill Rd. Adelphi, MD 20783-1145
1	Commandant U.S. Army Aviation School ATTN: Aviation Agency Fort Rucker, AL 36360
2	Program Manager U.S. Tank-Automotive Command ATTN: AMCPM-ABMS, T. Dean (2cps) Warren, MI 48092-2498
1	Project Manager U.S. Tank-Automotive Command Fighting Vehicle Systems ATTN: SFAE-ASM-BV Warren, MI 48397-5000
1	Project Manager, Abrams Tank System ATTN: SFAE-ASM-AB Warren, MI 48397-5000
1	Director HQ, TRAC RPD ATTN: ATCD-MA Fort Monroe, VA 23651-5143
2	Director U.S. Army Materials Technology Laboratory ATTN: SLCMT-ATL (2 cps) Watertown, MA 02172-0001
1	Commander U.S. Army Research Office ATTN: Technical Library P.O. Box 12211 Research Triangle Park, NC 27709-2211

No. of Copies	Organization
1	Commander U.S. Army Belvoir Research and Development Center ATTN: STRBE-WC Fort Belvoir, VA 22060-5006
1	Director U.S. Army TRAC-Ft. Lee ATTN: ATRC-L, Mr. Cameron Fort Lee, VA 23801-6140
1	Commandant U.S. Army Command and General Staff College Fort Leavenworth, KS 66027
1	Commandant U.S. Army Special Warfare School ATTN: Rev and Trng Lit Div Fort Bragg, NC 28307
3	Commander Radford Army Ammunition Plant ATTN: SMCAR-QA/HI LIB (3 cps) Radford, VA 24141-0298
1	Commander U.S. Army Foreign Science and Technology Center ATTN: AMXST-MC-3 220 Seventh Street, NE Charlottesville, VA 22901-5396
2	Commander Naval Sea Systems Command ATTN: SEA 62R SEA 64 Washington, DC 20362-5101
1	Commander Naval Air Systems Command ATTN: AIR-954-Tech Library Washington, DC 20360
1	Naval Research Laboratory Technical Library Washington, DC 20375
2	Commandant U.S. Army Field Artillery Center and School ATTN: ATSF-CO-MW, E.Dublisky Ft. Sill, OK 73503-5600

No. of Copies	Organization
1	Office of Naval Research ATTN: Code 473, R.S. Miller 800 N. Quincy Street Arlington, VA 22217-9999
3	Commandant U.S. Army Armor School ATTN: ATZK-CD-MS, M. Falkovitch (3 cps) Armor Agency Fort Knox, KY 40121-5215
2	Commander U.S. Naval Surface Warfare Center ATTN: J.P. Consaga C. Gotzmer Indian Head, MD 20640-5000
4	Commander Naval Surface Warfare Center ATTN: Code 730 Code R-13, K. Kim R. Bernecker H. Sandusky Silver Spring, MD 20903-5000
2	Commanding Officer Naval Underwater Systems Center ATTN: Code 5B331, R.S. Lazar Technical Library Newport, RI 02840
1	Director Benet Weapons Laboratories ATTN: SMCAR-CCB-RA, G.P. O'Hara Watervliet, NY 12189-4050
5	Commander Naval Surface Warfare Center ATTN: Code G33, J. East W. Burrell J. Johndrow Code G23, D. McClure Code DX-21 Tech Library Dahlgren, VA 22448-5000

No. of Copies	Organization
3	Commander Naval Weapons Center ATTN: Code 388, C.F. Price Code 3895, T. Parr Information Science Division China Lake, CA 93555-6001
1	OSD/SDIO/IST ATTN: L.H. Caveny Pentagon Washington, DC 20301-7100
4	Commander Indian Head Division Naval Surface Warfare Center ATTN: Code 610, T.C. Smith D. Brooks K. Rice Technical Library Indian Head, MD 20640-5035
1	AL/TSTL (Technical Library) ATTN: J. Lamb Edwards AFB, CA 93523-5000
1	AFATL/DLYV Eglin AFB, FL 32542-5000
1	AFATL/DLXP Eglin AFB, FL 32542-5000
1	AFATL/DLJE Eglin AFB, FL 32542-5000
1	AFELM, The Rand Corporation ATTN: Library D 1700 Main Street Santa Monica, CA 90401-3297
3	AAI Corporation ATTN: J. Hebert J. Frankle D. Cleveland P.O. Box 126 Hunt Valley, MD 21030-0126
2	Aerojet Solid Propulsion Co. ATTN: P. Micheli L. Torreyson Sacramento, CA 96813

No. of Copies | Organization

3 AL/LSCF
ATTN: J. Levine
L. Quinn
T. Edwards
Edwards AFB, CA 93523-5000

1 AVCO Everett Research Laboratory
ATTN: D. Stickler
2385 Revere Beach Parkway
Everett, MA 02149-5936

1 General Electric Company
Tactical System Department
ATTN: J. Mandzy
100 Plastics Ave.
Pittsfield, MA 01201-3698

1 IITRI
ATTN: M.J. Klein
10 W. 35th Street
Chicago, IL 60616-3799

1 Hercules, Inc.
Allegheny Ballistics Laboratory
ATTN: William B. Walkup
P.O. Box 210
Rocket Center, WV 26726

1 Hercules, Inc.
Radford Army Ammunition Plant
ATTN: E. Hibshman
Radford, VA 24141-0299

1 Hercules, Inc.
Hercules Plaze
ATTN: B.M. Riggleman
Wilmington, DE 19894

3 Lawrence Livermore National Laboratory
ATTN: L-355,
A. Buckingham
M. Finger
L-324, M. Constantino
P.O. Box 808
Livermore, CA 94550-0622

1 Olin Corporation
Badger Army Ammunition Plant
ATTN: F.E. Wolf
Baraboo, WI 53913

No. of Copies | Organization

3 Olin Corporation
ATTN: E.J. Kirschke
A.F. Gonzalez
D.W. Worthington
P.O. Box 222
St. Marks, FL 32355-0222

1 Olin Ordinance
ATTN: H.A. McElroy
10101 9th Street, North
St. Petersburg, FL 33716

1 Paul Gough Associates, Inc.
ATTN: P.S. Gough
1048 South St.
Portsmouth, NH 03801-5423

1 Physics International Company
ATTN: Library/H. Wayne Wampler
2700 Merced Street
San Leandro, CA 984577-5602

1 Princeton Combustion Research Laboratory, Inc.
ATTN: M. Summerfield
475 US Highway One
Monmouth Junction, NJ 08852-9650

2 Rockwell International
Rocketdyne Division
ATTN: BA08,
J. Flanagan
J. Gray
6633 Canoga Avenue
Canoga Park, CA 91303-2703

1 Thiokol Corporation
Huntsville Division
ATTN: Tech Library
Huntsville, AL 35807

1 Sverdrup Technology, Inc.
ATTN: Dr. John Deur
2001 Aerospace Parkway
Brook Park, OH 44142

2 Thiokol Corporation
Elkton Division
ATTN: R. Biddle
Tech Library
P.O. Box 241
Elkton, MD 21921-0241

No. of Copies | Organization

1 Veritay Technology, Inc.
ATTN: E. Fisher
4845 Millersport Hwy.
East Amherst, NY 14501-0305

1 Universal Propulsion Company
ATTN: H.J. McSpadden
25401 North Central Ave.
Phoenix, AZ 85027-7837

1 Battelle
ATTN: TACTEC Library, J.N. Huggins
505 King Avenue
Columbus, OH 43201-2693

1 Brigham Young University
Department of Chemical Engineering
ATTN: M. Beckstead
Provo, UT 84601

1 California Institute of Technology
204 Karman Lab
Main Stop 301-46
ATTN: F.E.C. Culick
1201 E. California Street
Pasadena, CA 91109

1 California Institute of Technology
Jet Propulsion Laboratory
ATTN: L.D. Strand, MS 512/102
4800 Oak Grove Drive
Pasadena, CA 91109-8099

1 University of Illinois
Department of Mechanical/Industry Engineering
ATTN: H. Krier
144 MEB; 1206 N. Green St.
Urbana, IL 61801-2978

1 University of Massachusetts
Department of Mechanical Engineering
ATTN: K. Jakus
Amherst, MA 01002-0014

1 University of Minnesota
Department of Mechanical Engineering
ATTN: E. Fletcher
Minneapolis, MN 55414-3368

No. of Copies | Organization

3 Georgia Institute of Technology School of Aerospace Engineering
ATTN: B.T. Zim
E. Price
W.C. Strahle
Atlanta, GA 30332

1 Institute of Gas Technology
ATTN: D. Gidaspow
3424 S. State Street
Chicago, IL 60616-3896

1 Johns Hopkins University
Applied Physics Laboratory
Chemical Propulsion Information Agency
ATTN: T. Christian
Johns Hopkins Road
Laurel, MD 20707-0690

1 Massachusetts Institute of Technology
Department of Mechanical Engineering
ATTN: T. Toong
77 Massachusetts Avenue
Cambridge, MA 02139-4307

1 Pennsylvania State University
Department of Mechanical Engineering
ATTN: V. Yang
University Park, PA 16802-7501

1 Pennsylvania State University
Department of Mechanical Engineering
ATTN: K. Kuo
University Park, PA 16802-7501

1 Pennsylvania State University
Assistant Professor
Department of Mechanical Engineering
ATTN: Dr. Stefan T. Thynell
219 Hallowell Building
University Park, PA 16802-7501

1 Pennsylvania State University
Director, Gas Dynamics Laboratory
Department of Mechanical Engineering
ATTN: Dr. Gary S. Settles
303 Mechanical Engineering Buidling
University Park, PA 16802-7501

No. of Copies | Organization

1 SRI International
Propulsion Sciences Division
ATTN: Tech Library
333 Ravenwood Avenue
Menlo Park, CA 94025-3493

1 Rensselaer Ploytechnic Institute
Department of Mathematics
Troy, NY 12181

2 Director
Los Alamos Scientific Lab
ATTN: T3/D. Butler
M. Division/B. Craig
P.O. Box 1663
Los Alamos, NM 87544

1 General Applied Sciences Lab
ATTN: J. Erdos
77 Raynor Ave.
Ronkonkama, NY 11779-6649

1 Battelle PNL
ATTN: Mr. Mark Garnich
P.O. Box 999
Richland, WA 99352

1 Stevens Institute of Technology
Davidson Laboratory
ATTN: R. McAlevy III
Castle Point Station
Hoboken, NJ 07030-5907

1 Rutgers University
Department of Mechanical and
Aerospace Engineering
ATTN: S. Temkin
University Heights Campus
New Brunswick, NJ 08903

1 University of Southern California
Mechanical Engineering Department
ATTN: 0HE200, M. Gerstein
Los Angeles, CA 90089-5199

No. of Copies | Organization

1 University of Utah
Department of Chemical Engineering
ATTN: A. Baer
Salt Lake City, UT 84112-1194

1 Washington State University
Department of Mechanical Engineering
ATTN: C.T. Crowe
Pullman, WA 99163-5201

1 Alliant Techsystems, Inc.
ATTN: R.E. Tompkins
MN38-3300
5700 Smetana Dr.
Minnetonka, MN 55343

1 Alliant Techsystems, Inc.
ATTN: J. Kennedy
7225 Northland Drive
Brooklyn Park, MN 55428

1 Science Applications, Inc.
ATTN: R.B. Edelman
23146 Cumorah Crest Drive
Woodland Hills, CA 91364-3710

1 Battelle Columbus Laboratories
ATTN: Mr. Victor Levin
505 King Ave.
Columbus, OH 43201-2693

1 Allegheny Ballistics Laboratory
Propulsion Technology Department
Hercules Aerospace Company
ATTN: Mr. Thomas F. Farabaugh
P.O. Box 210
Rocket Center, WV 26726

1 MBR Research Inc.
ATTN: Dr. Moshe Ben-Reuven
601 Ewing St., Suite C-22
Princeton, NJ 08540

Aberdeen Proving Ground

1 Cdr, CSTA
ATTN: STECS-PO/R. Hendricksen

INTENTIONALLY LEFT BLANK.

USER EVALUATION SHEET/CHANGE OF ADDRESS

This laboratory undertakes a continuing effort to improve the quality of the reports it publishes. Your comments/answers below will aid us in our efforts.

1. Does this report satisfy a need? (Comment on purpose, related project, or other area of interest for which the report will be used.) _____

2. How, specifically, is the report being used? (Information source, design data, procedure, source of ideas, etc.) _____

3. Has the information in this report led to any quantitative savings as far as man-hours or dollars saved, operating costs avoided, or efficiencies achieved, etc? If so, please elaborate. _____

4. General Comments. What do you think should be changed to improve future reports? (Indicate changes to organization, technical content, format, etc.) _____

BRL Report Number BRL-TR-3366 Division Symbol _____

Check here if desire to be removed from distribution list. ____

Check here for address change. ____

Current address: Organization _____
Address _____

DEPARTMENT OF THE ARMY
Director
U.S. Army Ballistic Research Laboratory
ATTN: SLCBR-DD-T
Aberdeen Proving Ground, MD 21005-5066

OFFICIAL BUSINESS

BUSINESS REPLY MAIL
FIRST CLASS PERMIT No 0001, APG, MD

Postage will be paid by addressee.

Director
U.S. Army Ballistic Research Laboratory
ATTN: SLCBR-DD-T
Aberdeen Proving Ground, MD 21005-5066

NO POSTAGE
NECESSARY
IF MAILED
IN THE
UNITED STATES